JGR Biogeosciences

RESEARCH ARTICLE
10.1029/2025JG008899

Special Collection:
Exploring Carbon Cycling in Aquatic Ecosystems Using Novel Analytical and Data-Driven Approaches

Key Points:

- Climate-induced landscape perturbations will lead to increased mobilization of terrestrial dissolved organic carbon (DOC) into Arctic rivers
- Shrubification, wildfires, and permafrost thaw will all impact the bioavailability of DOC in Arctic and sub-Arctic landscapes
- Aliphatic compounds are preferentially degraded by riverine microbes, leading to aromatic enrichment in downstream organic matter pools

Correspondence to:
A. E. Slentz,
aslentz@fsu.edu

Citation:
Slentz, A. E., McKenna, A. M., Kellerman, A. M., Holt, A. D., Burns, A. J., Miller, M. G., et al. (2025). Signatures of Arctic change: Molecular-level composition and bioavailability of shifting dissolved organic matter sources. *Journal of Geophysical Research: Biogeosciences*, *130*, e2025JG008899. https://doi.org/10.1029/2025JG008899

Received 28 FEB 2025
Accepted 5 JUL 2025

Signatures of Arctic Change: Molecular-Level Composition and Bioavailability of Shifting Dissolved Organic Matter Sources

A. E. Slentz[1], A. M. McKenna[2], A. M. Kellerman[1,3], A. D. Holt[1,4], A. J. Burns[5], M. G. Miller[6], S. Wagner[6], M. Tzortziou[7], H. Smith[8], A. Mannino[8], J. P. Chanton[1], and R. G. M. Spencer[1]

[1]National High Magnetic Field Laboratory Geochemistry Group and Department of Earth, Ocean, and Atmospheric Science, Florida State University, Tallahassee, FL, USA, [2]National High Magnetic Field Laboratory Ion Cyclotron Resonance Facility, Tallahassee, FL, USA, [3]Department of Earth and Environmental Science, University of Pennsylvania, Philadelphia, PA, USA, [4]Program on the Environment and Alaska Coastal Rainforest Center, University of Alaska Southeast, Juneau, AK, USA, [5]Department of Land and Water Resources, University of California, Davis, CA, USA, [6]Department of Earth and Environmental Sciences and Center for Environmental Stable Isotope Analysis, Rensselaer Polytechnic Institute, Troy, NY, USA, [7]Earth and Atmospheric Sciences Department, The City College of New York, New York, NY, USA, [8]Ocean Ecology Laboratory (Code 616), NASA Goddard Space Flight Center, Greenbelt, MD, USA

Abstract The Arctic is experiencing unprecedented rates of climate change, leading to numerous disturbances on the terrestrial landscape, including shrubification, increased frequency of wildfires, and permafrost thaw. These changes may impact the mobilization of terrestrial organic carbon into Arctic rivers and are hypothesized to lead to distinct alterations to the molecular composition and thus the reactivity of riverine dissolved organic matter (DOM). To understand how these three major perturbations may impact DOM dynamics in Arctic fluvial and coastal systems, we examined the concentration and bioavailability of dissolved organic carbon (DOC) together with the molecular-level DOM composition of different source endmember leachates from the Yukon River watershed using biodegradation incubation experiments and Fourier transform ion cyclotron resonance mass spectrometry (FT-ICR MS). Simulated climate-related landscape perturbations generally led to increased leachate DOC concentrations. Incubations demonstrated that the biodegradability of leachate DOC was lowest for vegetation endmembers, particularly for shrubs (12.3% DOC loss), and highest for thawing Yedoma permafrost (64.9% loss) and organic-rich tundra soil (70.9% loss). FT-ICR MS highlighted that aliphatic and high-H/C molecular formulas were preferentially biodegraded, whereas condensed aromatic and polyphenolic compounds were relatively enriched post-biodegradation in all endmember leachates. Together these findings suggest that with continued climate change and landscape perturbation, larger amounts of less bioavailable DOC will be mobilized into Arctic rivers leading to higher relative amounts of highly aromatic, biologically stable DOM being exported into receiving ecosystems and the Arctic Ocean, potentially altering the rates and mechanisms of carbon turnover in the coastal zone.

Plain Language Summary The Arctic landscape is undergoing major widespread perturbations due to amplified impacts of climate change. These landscape alterations, including shifting dominant plant communities, more frequent and severe wildfires, and permafrost thaw are expected to alter Arctic carbon cycling via shifts in the quantity and quality of dissolved organic matter (DOM) transported into rivers, affecting both local and downstream biogeochemistry. However, changes to riverine DOM composition and reactivity due to Arctic amplification are not well-constrained. We employed biodegradation incubations of leachates from a variety of vegetation and soil endmembers in addition to ultrahigh resolution mass spectrometry to: (a) improve the quantification of terrestrial dissolved organic carbon mobilized into Arctic rivers with respect to shifting sources, (b) determine potential changes in DOM bioavailability with continued landscape alteration, and (c) contextualize DOM bioavailability with changes in molecular composition. Results indicated that climate-induced landscape alterations may lead to higher amounts of less bioavailable terrestrial DOM being mobilized into Arctic rivers, leading to an accumulation of DOM rich in aromatic compounds in downstream reservoirs due to selective biodegradation of aliphatic and other high-H/C molecular formulas.

1. Introduction

The Arctic ecosystem is among the most vulnerable on Earth to global climate change (Moon et al., 2024). Surface air temperatures in northern high-latitude regions have increased at more than double the rate of other parts of the planet since the beginning of the 21st century leading to numerous major landscape alterations throughout the region (Box et al., 2019; Meredith et al., 2019; Rantanen et al., 2022). In particular, Arctic and sub-Arctic tundra ecosystems are experiencing dramatic changes as a result of rapid warming, such as increased shrub area coverage, height, and biomass, a phenomenon colloquially known as "shrubification" (Berner & Goetz, 2022; Frost et al., 2024; Mekonnen et al., 2021), increased susceptibility to wildfires (McCarty et al., 2020; Veraverbeke et al., 2021), and rapid thawing of underlying permafrost (Miner et al., 2022; Schuur et al., 2008, 2015). Each of these terrestrial perturbations have ramifications for Arctic and sub-Arctic carbon dynamics.

The rate of shrub expansion into northern high-latitudes has increased in recent decades ranging from 10 to 100 m yr^{-1} (Rees et al., 2020). Species such as dwarf birch, willow, alder, and evergreen shrubs are expected to dominate tundra landscapes by the end of the century (Mekonnen et al., 2018). This shift corresponds with an overall decrease in species diversity as obligate herbaceous and nonvascular tundra species (e.g., sedges and grasses, mosses, and lichens) are outcompeted (Chapin et al., 1995, 1996; Mod & Luoto, 2016; Wilson & Nilsson, 2009) resulting in an increase in primary productivity and overall carbon sequestration (Natali et al., 2012). Shrubification, along with extreme temperatures, drier conditions, and severe weather (e.g., lightning), has also led to increased fuel availability and surface flammability in boreal forests and tundra landscapes leading to increased vulnerability to wildland fires (McCarty et al., 2020, 2021). Although wildfires have been largely absent in the Arctic throughout the Holocene, fire activity in several Arctic regions has increased by up to three-fold since the late-20th century (Kharuk et al., 2022; McCarty et al., 2021). Between 2001 and 2020, wildland fires in Arctic-boreal ecosystems emitted an average of 142 Tg C yr^{-1} and were the most significant source of black carbon (i.e., soot and other charred residues) at latitudes above 60°N (McCarty et al., 2021; Veraverbeke et al., 2021). Although wildfires have served as major sources of carbon to the atmosphere in recent years, permafrost thaw has been identified as one of the most prolific threats to the ecosystem carbon balance in the Arctic (e.g., Schuur et al., 2008, 2015; Zimov et al., 2006). Permafrost serves as a major reservoir of terrestrial organic carbon (~1,500 Pg C) storing more than twice the amount of current atmospheric carbon (Schuur et al., 2015). The release of even a small fraction of the permafrost carbon reservoir as methane and carbon dioxide via microbial respiration can have severe implications for future climate warming (Schuur et al., 2008, 2015). It is estimated that by the year 2100, the pan-Arctic region will experience a 30%–70% loss of near-surface permafrost (Lawrence et al., 2012). This reduction in permafrost extent is projected to increase permafrost CO_2 emissions by up to 41%, effectively offsetting any increases in carbon uptake by shifting vegetation communities, making the tundra ecosystem a net carbon source (Natali et al., 2014, 2024).

Despite the abundance of information surrounding shifts in inorganic carbon fluxes associated with the changing Arctic landscape (e.g., Drake et al., 2015, Drake, Tank et al., 2018; Schuur et al., 2015; Tank et al., 2023), long-term impacts of climate-induced shrubification, shifting wildfire regimes, and permafrost thaw on organic carbon export and cycling in northern high-latitude fluvial systems are largely understudied. Dissolved organic carbon (DOC) serves as a key substrate for microbial heterotrophic respiration and thus plays an important regulatory role for ecosystem CO_2 production (Drake et al., 2015, Drake, Guillemette, et al., 2018; Tranvik et al., 2009). DOC comprises the quantifiable fraction of dissolved organic matter (DOM), which represents a complex mixture of an extremely diverse suite of organic compounds, the composition of which reflects its source material, and the history of its biogeochemical transformations (Kellerman et al., 2014; Stubbins et al., 2010). Because distinct sources of DOM each display unique chemical signatures (Kellerman et al., 2018), changes in external sources via perturbations of the terrestrial landscape can lead to substantial shifts in the molecular composition of riverine DOM, which is intrinsically tied to its reactivity and ecological function (D'Andrilli et al., 2015; Hernes et al., 2017; Holmes et al., 2013; Johnston et al., 2019; Kellerman et al., 2015). The amplification of climate change and resultant perturbations to Arctic ecosystems highlight the importance of understanding how environmental drivers such as shrubification, wildfires, and permafrost thaw will alter the quantity, quality, and thus reactivity of riverine DOM exported from Arctic landscapes and their cumulative effects on carbon cycling downstream and in coastal and marine systems (Grunert et al., 2021; McClelland et al., 2012).

Major alterations to terrigenous DOM inputs are of particular concern in Arctic fluvial systems due to the relatively small size of the receiving Arctic Ocean, which comprises only ~1% of the global ocean by volume yet

receives >10% of global river discharge (Holmes et al., 2012; McClelland et al., 2012). The high volume of freshwater exported into the Arctic Ocean is accompanied by an estimated DOC flux of 34–40 Tg C yr^{-1} from the pan-Arctic watershed (Holmes et al., 2012; Johnston et al., 2018; Starr et al., 2023), most of which is terrestrially derived (Amon et al., 2012; Spencer et al., 2008). The mobility and processing of this DOM varies, and it may be mineralized by microbial or photochemical processes within the river or be preserved and transported to the Arctic Ocean where it may impact biogeochemical cycles and physicochemical properties in coastal environments. Since the composition of DOM, in part, controls its reactivity and fate, it is fundamentally important to understand how the impacts of climate change on the landscape will manifest in the quantity and composition of DOM mobilized from land to the ocean (McClelland et al., 2012).

In this study, we utilized the unparalleled mass accuracy and precision of 21T Fourier transform ion cyclotron resonance mass spectrometry (FT-ICR MS) to examine the DOM molecular signatures of leachates from a suite of vegetation and soil material that represent different biomass endmembers and DOM sources in the Yukon River watershed chosen to exemplify three major climate-related changes to Arctic and sub-Arctic landscapes: tundra shrubification (Bellard et al., 2012; Elmendorf et al., 2012), shifting wildfire regimes (McCarty et al., 2021), and permafrost thaw (Schuur et al., 2015). In addition to examining how molecular-level composition may change with shifting sources in high-latitude terrestrial environments, we also investigated ramifications for DOC concentrations and bioavailability of the different endmembers through bioincubation experiments to assess environmental fate. Finally, we analyzed molecular-level shifts in composition pre- and post-bioincubation to examine links between DOM composition and biodegradability in aquatic environments. We use the compositional insights gained through endmember leachate bioincubations to postulate impacts of continued perturbation of the Arctic and sub-Arctic landscape on terrestrial DOC fluxes and the biogeochemistry of receiving aquatic ecosystems.

2. Materials and Methods

2.1. Study Location

Within the Arctic, the Yukon River represents one of the largest inputs of organic carbon to the Arctic Ocean. The Yukon River drains an area of 830,000 km^2 throughout Alaska (USA) and Canada's Yukon Territory and British Columbia and is the fifth largest Arctic river by annual discharge (208 km^3 yr^{-1}; Holmes et al., 2012). Discharge to the receiving Bering Sea and, subsequently, to the Arctic Ocean is characterized by strong seasonal fluctuations with high concentrations of DOC in the spring typically declining through the summer to low DOC concentrations in the winter months (Behnke et al., 2021). The Yukon River watershed is largely underlain by discontinuous permafrost, and dominant land cover classes in the region include grasslands (~40%), forests (~20%), shrublands (~20%), and wetlands (~8%; Amon et al., 2012). Although broadleaf and needleleaf forests dominate the landscape in the Yukon River's upper catchment, shrubs, moss hummocks, lichens, and herbaceous vegetation become more predominant in the lower delta region of interest (O'Donnell et al., 2010).

2.2. Sample Collection

A suite of model source endmember samples was chosen to represent the major climate-driven landscape alterations threatening the Arctic and sub-Arctic regions (i.e., tundra shrubification, changing wildfire regimes, and permafrost thaw) inclusive of several functional types of vegetation, burn products, and permafrost, mineral, and organic-rich soil types (Table 1). Endmember samples (n = 13) were collected from four sites with varying landcover types (i.e., moist sedge meadow floodplain, site ii; willow shrubland floodplain, site iii; high-bank shrub-tussock tundra, site iv; and burned mossy tundra, site v) throughout the Yukon River delta near Alakanuk (Alaska, USA) in August/September 2022 and June 2023 (Figure 1). Additionally, frozen Yedoma permafrost soil was collected initially as a part of Drake et al. (2015) from the Fox Permafrost Tunnel (Cold Regions Research and Engineering Laboratory; Fairbanks, Alaksa, USA; Figure 1a, site i). Yedoma permafrost is prevalent throughout the Yukon River basin (Strauss et al., 2021); as such, this endmember was sampled to represent the dominant permafrost type found in the Yukon River delta.

All fresh vegetation and soil endmembers (i.e., samples A–F, I–L; Table 1) were collected in August/September 2022, as this time of year represents the transition from summer to winter months, the period during which fresh inputs to the litter layer occur (Spencer et al., 2008). The char samples (i.e., G–H, N; Table 1) were collected in June 2023 from the site of the 2022 Apoon Pass fire, which represents one of the largest wildfires in the area to

Table 1
Model Source Endmember Name, ID, Sampling Location, and Functional Type With Corresponding Mean Leachate Dissolved Organic Carbon (DOC) Concentration, ΔDOC Over 28 Days, and Percent of Biodegradable DOC (%BDOC)

ID	Sample name	Sample site	Sample functional type	$[DOC]_0$ (mg C L^{-1})	ΔDOC (mg C L^{-1})	%BDOC
A	*Alnus sp.*	iii	shrub	618.3	41.2	6.7
B	*Salix sp.*	iii	shrub	962.1	173.0	18.0
C	*Carex sp.*	ii	graminoid	649.4	215.9	33.3
D	*Arctagrostis latifolia*	iv	graminoid	151.2	59.9	39.6
E	*Sphagnum sp.*	iv	obligate tundra vegetation	166.9	68.5	41.0
F	*Cladonia rangiferina*	iv	obligate tundra vegetation	107.2	54.5	50.8
G*	Charred Wood	v	shrub, charred	12.0	4.8	40.1
H*	Charred Moss	v	obligate tundra vegetation, charred	40.9	24.4	59.8
I	Floodplain Mud	ii	soil	2.7	1.3	46.3
J	Active Layer	iii	soil	2.2	1.1	52.3
K	Litter Layer	iii	soil	4.6	2.0	44.6
L	Tundra Soil	iv	soil	8.7	6.2	70.9
M	Yedoma permafrost	i	permafrost	16.3	10.6	64.9
N*	Charred Soil	v	soil, charred	17.1	6.6	38.6

Note. Asterisks (*) denote char samples.

date with a burn area of more than 360 km^2 (Figure 1b, site v). Although leaves were collected from each of the live plants sampled, burned vegetation endmembers were collected as litter. Active layer soils were sampled as a 10 cm^2 core taken at a depth of 0–10 cm below the litter layer, which was also sampled. Woody and other debris were removed from permafrost samples prior to homogenization (i.e., hand-mixing of several samples and establishing general uniformity) and storage (Drake et al., 2015). Upon collection all source endmember samples were placed into individual sterile freezer bags and stored frozen in the dark at −20°C until further processing.

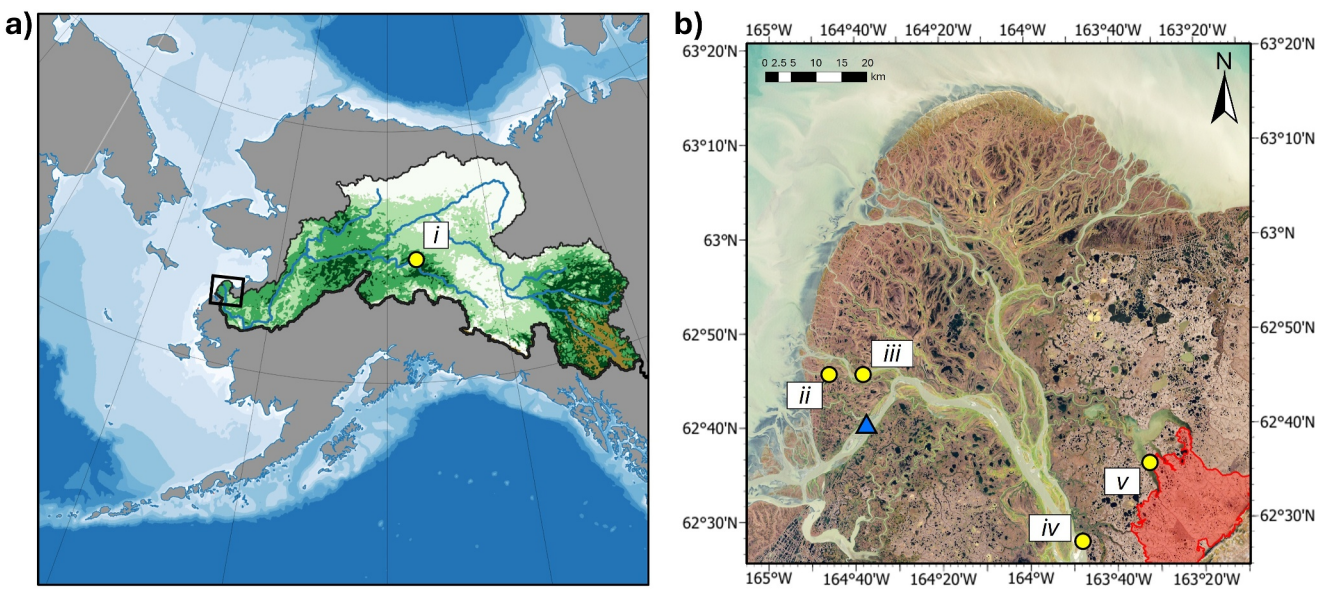

Figure 1. (a) Map of the Yukon River watershed (colored polygon) within the North American Arctic, and the main region sampled for endmembers (enclosed in black square). The permafrost sample was taken to the east (yellow circle, site i). (b) The region enclosed by the black square magnified with terrestrial endmembers (labeled yellow circles) and riverine inoculum (blue triangle) sampling locations plotted. Endmember sampling locations are labeled as follows: site ii (moist sedge meadow floodplain), site iii (willow shrubland floodplain), site iv (high-bank shrub-tussock tundra), and site v (burned mossy tundra). The shaded red area denotes the burn extent of the 2022 Apoon Pass fire.

A 2 L bulk river water sample to serve as the riverine inoculum was obtained from the Yukon River (62.67567°N, −164.62123°W) and utilized in all biodegradation incubations (Figure 1b). It was collected during the spring freshet (June 2023), the period with the greatest terrestrial DOM inputs due to the peak surface runoff (Behnke et al., 2021; Burns et al., 2024; Spencer et al., 2008). The sample was filtered through pre-combusted (450°C, 4 hr) Whatman GF/D (2.7 μm) filters and collected in an acid-washed (10% HCl v/v), polycarbonate bottle. This water sample was kept cold (4°C) and in the dark until bioincubation experiment setup (Textor et al., 2019; Wickland et al., 2012).

2.3. Leachate Preparation

Leachates of source endmembers were prepared according to established methods as described previously (Textor et al., 2019). The endmembers were divided into two groups with slightly varying preparation protocols: soil endmembers and vegetation endmembers. Although soil endmembers were kept frozen and left in field-moist conditions until leaching (Drake et al., 2015; Textor et al., 2019), all vegetation endmembers, including char, were thawed overnight and dried for 24 hr at 50°C. Once each endmember had been appropriately prepared for leaching, the solid endmember was added to a 1 L acid-washed high-density polyethylene Nalgene bottle and mixed with 1 mM $NaHCO_3$ buffering solution to a ratio of 1 g of solid per 100 mL of solution (Wickland et al., 2007). These mixtures were agitated on a shaker table (200 rpm) and leached for 24 hr in the dark at 22°C. Following this, solid substrates were separated from the leachate by filtering first through a DI-washed copper mesh sieve and then through a precombusted (450°C, >5 hr) Whatman GF/F (0.7 μm) filter using a filter tower and hand vacuum pump and finally through a 0.45 μm Geotech High-Capacity dispos-a-filter™ capsule filter.

2.4. Endmember Leachate Bioincubations

To assess the environmental fate of terrigenous DOM within the Yukon River system, the soil and vegetation leachates were subjected to biodegradation incubations conducted in the dark at room temperature (22°C) for 28 days. Samples were analyzed for DOC concentration at time steps of 0, 2, 7, 14, and 28 days to assess bioavailability and molecular composition pre- and post-bioincubation (i.e., 0 and 28 days). Filtered leachates were amended with 1% (v/v) of the Yukon River microbial inoculum to initiate the bioincubation (Vonk et al., 2015; Wickland et al., 2012). Triplicate 30 mL samples of each of the inoculated solutions for each of the five time points were immediately decanted into precleaned (10% HCl v/v, 48 hr) and precombusted (550°C, 5 hr) amber glass vials (40 mL) capped with plastic lids and sealed with cleaned (10% HCl v/v, 48 hr) Teflon-coated septa. To end the biodegradation at each time step, triplicate samples were filtered to 0.45 μm using Whatman GD/X PES syringe filters (Textor et al., 2019) and then acidified to a pH of 2 using reagent grade concentrated HCl and stored in the dark at 4°C until analysis. Additional samples were prepared for molecular-level compositional analysis via FT-ICR MS at initial and final time steps; inoculated leachates were decanted into two 125 mL pre-cleaned (10% v/v/HCl, 48 hr) polycarbonate bottles. Samples were filtered as previously described and stored frozen (−20°C) until further analysis.

2.5. Bulk Dissolved Organic Carbon Analysis

Filtered and acidified samples were analyzed for DOC concentrations on a Shimadzu TOC-L_{CPH} high-temperature catalytic oxidation total organic carbon analyzer (Shimadzu Corp., Kyoto, Japan) following established protocols (e.g., Johnston et al., 2019; Kellerman et al., 2023; Kurek et al., 2022; Stubbins & Dittmar, 2012). The nonpurgeable organic carbon (i.e., DOC) concentration was calculated based on the mean of three of up to seven replicate injections with a coefficient of variance <2% taken after 8 min of sparging with compressed air at a flow rate of 80 mL min^{-1}.

DOC loss (ΔDOC) was calculated as the difference between the initial ($t = 0$) and final ($t = 28$) concentrations for each endmember leachate.

$$(\Delta\mathrm{DOC}) = (\mathrm{DOC})_{\mathrm{initial}} - (\mathrm{DOC})_{\mathrm{final}} \quad (1)$$

The proportion of the bulk DOC that was bioavailable (%BDOC) was calculated as follows:

$$\%\mathrm{BDOC} = \left((\Delta\mathrm{DOC})/(\mathrm{DOC})_{\mathrm{initial}}\right) \times 100 \quad (2)$$

2.6. DOM Composition Sample Preparation by Solid-Phase Extraction

Pre- and post-bioincubation samples were thawed in the dark at 22°C, an aliquot of which was acidified with HPLC reagent grade HCl to pH = 2. Using a modified version of the solid-phase extraction procedure described by Dittmar et al., 2008, the prepared samples were extracted onto 100 mg bed, 3 mL volume Bond-Elut PPL columns (Agilent Technologies Inc., Santa Clara, CA). The volume of sample extracted was adjusted dependent upon the DOC concentration of the sample with a target column loading of 40 μg C. Prior to extraction, PPL columns were prepared as follows: cartridge contents were soaked with HPLC grade MeOH (>4 hr) followed by rinses with ultrapure water, MeOH, and pH 2 ultrapure water. Following sample extraction, cartridges were dried with a flow of ultrahigh purity nitrogen gas and eluted with 1 mL of HPLC grade MeOH into 2 mL precleaned (10% HCl v/v 48 hr) and combusted (550°C, 5 hr) amber glass vials. Samples were stored at −20°C until analysis by FT-ICR MS.

2.7. Dissolved Organic Matter Composition via Fourier Transform Ion Cyclotron Resonance Mass Spectrometry

Methanol eluates were analyzed without further modification for DOM composition in negative mode electrospray ionization (typical ion formation conditions: emitter voltage: −2.8–3.2 kV; S-lens RF level: 40% and heated metal capillary temperature: 350°C) with a custom-built hybrid linear ion trap FT-ICR mass spectrometer equipped with a 21T superconducting solenoid magnet (Hendrickson et al., 2015; Smith et al., 2018). Sample solutions were infused via a microelectrospray source (50 μm i. d. fused silica emitter) at 500 nL min^{-1} by a syringe pump (Emmett et al., 1998). Individual time-domain transients of 3.1 s were conditionally co-added and acquired with the Predator data station with 75 time-domain transients averaged for each experiment (Blakney et al., 2011). Mass spectra were phase-corrected (Xian et al., 2010) and internally calibrated with 10–15 highly abundant homologous series that spanned the entire molecular weight distribution (170–1,000 Da) based on the "walking" calibration method (Savory et al., 2011). Experimentally measured masses were converted to the Kendrick mass scale (Kendrick, 1963) for rapid identification of homologous series for each heteroatom class (i.e., species with the same $C_cH_hN_nO_oS_s$ content different only by degree of alkylation; Hughey et al., 2001). Peaks with signal magnitude greater than six times the baseline root-mean square noise at m/z 400 were exported to peak lists, and molecular formula assignments and data visualization were performed with PetroOrg software (Bahureksa et al., 2022; Corilo, 2014; Kim et al., 2003).

Molecular formulas were assigned to ions constrained by $C_{4–75}H_{4–150}O_{1–30}N_{0–4}S_{0–2}$. For all mass spectral data presented herein, 7,132–16,406 peaks were assigned elemental compositions (error ± 0.3 ppm). The modified aromaticity index (AI_{mod}; a robust proxy for aromaticity) and nominal carbon oxidation state (NOSC) were calculated for each formula according to Koch and Dittmar (2006, 2016) and Boye et al. (2017), respectively. Stoichiometric ratios (H/C, O/C, N/C, and S/C) were calculated, and formulas were grouped based on their heteroatom content (CHO, CHON, CHOS, and CHONS). Molecular formulas were also grouped into operational compound classes based on elemental ratios (H/C and O/C) and AI_{mod}: condensed aromatics (CA; $AI_{mod} > 0.67$), polyphenolics (PPh; $0.50 < AI_{mod} < 0.67$), highly unsaturated and phenolic (HUPs; $AI_{mod} < 0.50$, $H/C < 1.5$), and aliphatic ($H/C > 1.5$; Šantl-Temkiv et al., 2013). The relative abundance (RA) of each assigned formula was determined by expressing its peak intensity as a proportion of the total intensity of all assigned peaks in the sample, and the %RA of each heteroatom and operational compound class was calculated by summing the RA of all peaks belonging to the respective class.

2.8. Statistical Analysis

Data analysis was performed in RStudio (version 4.3.0), and Microsoft Excel and figures were made using ggplot2 and Microsoft Excel (Wickham, 2016). The two-tailed T-test function (T.test) in Excel was used to assess statistical significance between endmembers leachate DOC and biodegradability. Principal component analysis (PCA) was conducted using the FactorMine *R* package and was used to examine and visualize relationships between DOC biodegradability and changes in molecular-level DOM composition (i.e., FT-ICR MS parameters) pre- and post-bioincubation with variables scaled to unit variance to make them comparable (Lê et al., 2008). Specifically, the PCA considered %BDOC together with changes in RA-weighted mass, NOSC, AI_{mod} and atomic ratios (H/C, O/C, N/C, S/C) as well as heteroatom %RA (CHO, CHON, CHOS, and CHONS) and operational compound class %RA (CA, PPh, HUPs, and aliphatics) associated with each leachate.

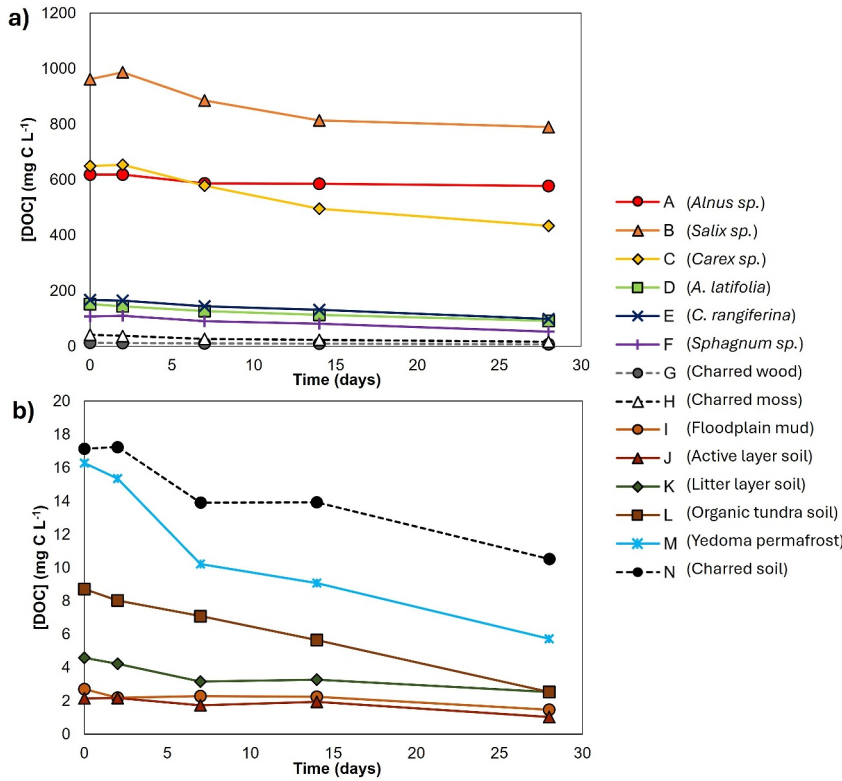

Figure 2. Endmember leachate dissolved organic carbon concentrations at each bioincubation time step (0, 2, 7, 14, and 28 days). Endmembers are grouped by functional type: (a) vegetation (samples A–H) and (b) soils (samples I–N). Dotted lines indicate char samples.

3. Results

3.1. Concentration and Bioavailability of Source-Specific Dissolved Organic Carbon

Initial DOC concentrations from source endmember leachates spanned more than two orders of magnitude ranging from 2.2 to 962.1 mg C L^{-1} (Table 1). Of the endmember functional types studied (i.e., vegetation, soils, char, and permafrost), vegetation samples had the highest DOC concentrations ranging from 107.2 to 962.1 mg C L^{-1} (Table 1, Figure 2a). Shrub leachates (samples A and B) were at the upper end of this range (mean = 790.2 mg C L^{-1}), followed by graminoids (samples C and D; mean = 400.3 mg C L^{-1}), with the lower end of the DOC range occupied by obligate tundra species (mosses and lichens, samples E and F; mean = 137.1 mg C L^{-1}; Table 1, Figure 2a). Overall, vegetation endmembers leached significantly more DOC than soils ($p < 0.05$), whose leachate DOC concentrations ranged between 2.2 and 16.3 mg C L^{-1} (Table 1, Figure 2b). Mineral soils (samples I–K) leached 63.9 ± 14.6% less DOC than organic-rich tundra soil (sample L) and 86.0 ± 4.7% less than permafrost (sample M; Table 1, Figure 2b). DOC yields from charred endmembers did not follow a clear trend in comparison with their fresh counterparts. For example, charred moss (sample H) leached an initial DOC concentration of 40.9 mg C L^{-1} in comparison to fresh *Sphagnum* (sample E), which yielded 166.9 mg C L^{-1} upon leaching (Table 1). Conversely, charred tundra soil (sample N; 17.1 mg C L^{-1}) yielded more DOC upon leaching than fresh tundra soil (sample L; 8.7 mg C L^{-1}; Table 1, Figure 2).

Bioavailability over the course of the incubation experiments similarly exhibited vast differences between individual leachates and endmember functional types with %BDOC ranging from 6.7% to 70.9% (Table 1, Figure 3). In general, soil leachate DOC was the most bioavailable and vegetation leachate DOC was the most biologically stable with char leachates falling in the middle (Table 1, Figure 3). The organic tundra soil experienced the greatest loss in DOC via biodegradation (70.9% BDOC), followed by permafrost (64.9% BDOC), mineral soils (47.8 ± 4.0% BDOC), charred endmembers (46.1 ± 11.8% BDOC) obligate tundra species

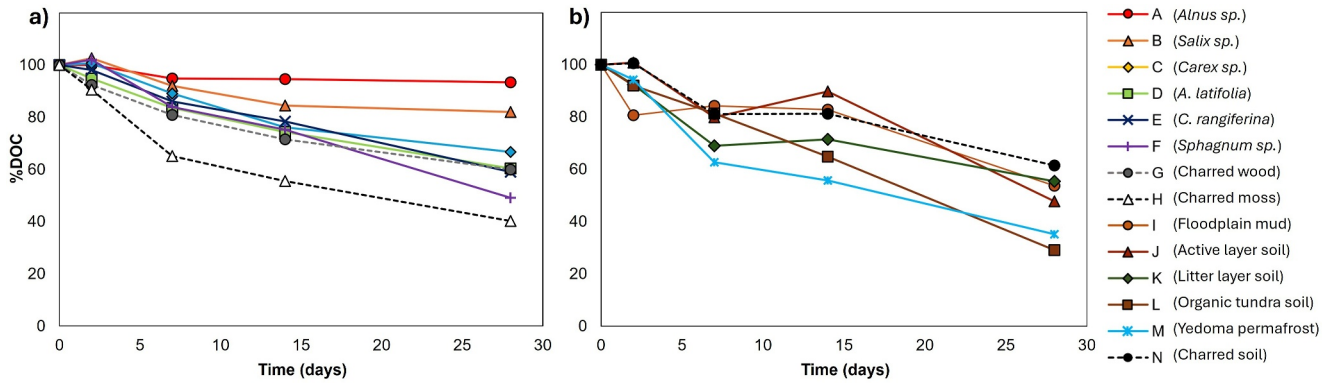

Figure 3. Mean percent dissolved organic carbon remaining (i.e., 1 − BDOC) for each sample at each time step (0, 2, 7, 14, and 28 days) normalized to the same starting point. Endmembers are grouped by functional type: (a) vegetation (samples A–H) and (b) soils (samples I–N). Dotted lines indicate char samples.

(45.9 ± 7.0% BDOC), graminoids (36.4 ± 4.5% BDOC), and finally shrubs (12.3 ± 8.0% BDOC; Table 1, Figure 3).

3.2. Molecular Composition of Endmember Leachate Dissolved Organic Matter

Although the molecular-level DOM composition was unique to each source endmember, DOM composition was initially dominated by HUPs formulas across all samples (46.3–82.0%RA, mean = 62.3%RA; Table 2; Figure 4a). Aliphatic (4.4–35.0%RA, mean = 16.7%RA) and PPh (4.7–26.6%RA, mean = 16.2%RA) molecular formulas were comparable in average RA, and CA molecular formulas were the least abundant (0.8–10.2%RA, mean = 4.8%RA; Table 2, Figure 4a). AI_{mod} values ranged between 0.24 (sample E, *Sphagnum* moss) and 0.40 (sample F, *C. rangiferina*; sample L, organic-rich tundra soil; Table 2). Average endmember NOSC was −0.07 with the lowest oxidation state exhibited by permafrost (sample M; −0.37) and the highest by alder (sample A, 0.07; Table 2). The mean stoichiometric ratio of H/C for all endmembers was 1.11 ± 0.09 with the highest value from permafrost (sample M; 1.27) and the lowest by other soils (samples I–L; 1.05 ± 0.05; Table 2). Heteroatom composition was dominated by CHO-containing formulas (72.5–97.6%RA, mean = 82.7%RA) followed by CHON-containing formulas (2.0–23.6%RA, mean = 11.7%RA), CHOS-containing formulas (0.3–15.5%RA, mean = 5.6%RA), and CHONS-containing formulas having the lowest RA (0–0.02%RA, mean = 0.001%RA; Table 2, Figure 5a). Samples E (*Sphagnum* moss), G (charred wood), and L (tundra soil) were the most enriched in N-containing formulas, whereas samples I–K (mineral soils) and M (permafrost) were the most enriched in S-containing formulas (Table 2, Figure 5a).

There were several notable changes in DOM molecular composition as a result of the 28-day biodegradation experiments (Figure 4). Principally, aliphatic molecular formulas were preferentially degraded with all but two samples (B and C, *Salix* sp. and *Carex* sp., respectively) exhibiting a loss in RA of this compound class (−1.9 to −28.2%RA, mean = −8.3%RA; Table 2, Figure 4b). This loss in aliphatic content was most notable in the soil endmembers (mean = −13.0%RA) followed by charred endmembers (mean = −4.4%RA) and the least prevalent in vegetation endmembers (mean = −2.6%RA). *Salix* sp. and *Carex* sp. (samples B and C, respectively) exhibited a relative increase in aliphatic content accompanied by a relative decrease (−12.2%RA) in HUPs molecular formulas (Table 2, Figure 4b). A loss in RA of HUPs molecular formulas was observed in over half of the endmembers, though there was no discernible trend among endmember functional types (Figure 4). This was likely a result of loss of high-H/C HUP molecular formulas, specifically, as the average H/C across all endmembers decreased from 1.11 preincubation to 1.01 postincubation (Table 2). In general, the relative contribution of PPh (0.3–15.0%RA, mean = 6.2%RA) and CA (−0.1–7.7%RA, mean = 2.5%RA) increased relative to the decrease in higher H/C compounds. AI_{mod}, and thus overall aromaticity, increased over the course of bio-incubation experiments (T0 mean = 0.33, T28 mean = 0.38; Table 2) with the most notable increase exhibited by char samples (+0.07; Table 2). Reflecting the greater degree of processing postincubation, average NOSC also largely increased due to biodegradation of endmember leachates (mean = +0.11; Table 2) with the highest endpoint and greatest increases in oxidation states demonstrated by soils (0.21, +0.31, respectively; Table 2), whereas vegetation endmember leachates retained much lower oxidation states despite degradation (T28 mean

Table 2

FT-ICR MS Properties of Each Model Source Endmember Before Biodegradation (t = 0) and After (t = 28), Including Average Mass, AI_{mod} (Modified Aromaticity Index), NOSC (Nominal Oxidation State of Carbon), Stoichiometric Ratios, and the Percent Relative Abundance (%) of Heteroatom Content and Operational Compound Classes (CA = Condensed Aromatic, PPh = Polyphenolic, HUP = Highly Unsaturated and Phenolic, Aliph = Aliphatic)

ID	Time-point	Mass	AI_{mod}	NOSC	CHO (%)	CHON (%)	CHOS (%)	CHONS (%)	H/C	O/C	N/C	S/C	CA (%)	PPh (%)	HUP (%)	Aliph (%)
A	0	502.57	0.38	0.07	97.6	2.0	0.3	0.0	1.01	0.53	0.00	0.00	7.1	18.9	63.0	10.9
	28	488.24	0.41	0.09	92.6	4.1	3.3	0.0	0.97	0.53	0.00	0.00	10.6	22.0	58.4	9.0
B	0	505.16	0.28	−0.05	90.1	4.7	5.2	0.0	1.16	0.55	0.00	0.00	1.4	4.7	73.6	20.3
	28	487.10	0.30	−0.18	83.0	3.6	13.4	0.0	1.16	0.48	0.00	0.01	4.0	11.5	60.5	24.1
C	0	534.95	0.30	−0.01	85.2	11.7	3.1	0.0	1.12	0.54	0.01	0.00	1.2	8.4	76.4	14.0
	28	495.07	0.32	−0.13	72.7	19.1	7.9	0.3	1.13	0.47	0.02	0.00	2.7	16.3	65.1	15.9
D	0	468.42	0.28	−0.21	82.9	11.9	5.2	0.0	1.20	0.48	0.01	0.00	1.8	12.7	62.9	22.6
	28	457.11	0.33	−0.20	78.1	13.7	8.2	0.0	1.14	0.45	0.01	0.00	2.9	18.1	61.7	17.3
E	0	445.80	0.24	−0.30	72.5	23.6	3.9	0.0	1.29	0.45	0.03	0.00	1.6	11.9	51.5	35.0
	28	472.03	0.28	−0.16	76.5	20.8	2.7	0.0	1.19	0.49	0.02	0.00	2.2	15.1	60.2	22.4
F	0	441.98	0.40	−0.02	90.0	9.6	0.4	0.0	1.01	0.48	0.01	0.00	0.8	12.8	82.0	4.4
	28	423.17	0.42	0.07	93.9	5.0	1.1	0.0	0.98	0.52	0.00	0.00	0.7	13.8	82.7	2.9
G*	0	477.90	0.34	0.00	79.8	17.6	2.6	0.0	1.08	0.52	0.01	0.00	4.6	15.6	72.4	7.4
	28	483.98	0.38	0.04	77.7	18.1	3.8	0.4	1.02	0.51	0.01	0.00	7.4	21.1	67.0	4.5
H*	0	509.65	0.35	0.07	86.1	11.8	2.1	0.0	1.05	0.55	0.01	0.00	3.7	14.6	71.9	9.8
	28	500.46	0.43	0.13	87.0	9.3	3.7	0.0	0.94	0.53	0.01	0.00	11.4	29.7	52.5	6.4
I	0	446.41	0.36	−0.11	77.1	11.7	11.1	0.0	1.09	0.47	0.01	0.01	8.1	23.2	50.0	18.7
	28	491.65	0.41	0.16	78.0	15.2	6.8	0.0	0.96	0.54	0.01	0.00	9.9	27.4	52.5	10.1
J	0	453.00	0.38	0.05	76.1	11.0	13.0	0.0	1.03	0.52	0.01	0.01	9.4	24.6	49.8	16.3
	28	494.82	0.40	0.21	78.4	14.6	7.0	0.0	0.96	0.57	0.01	0.01	10.0	24.9	58.5	6.6
K	0	439.56	0.37	−0.14	76.5	11.0	12.6	0.0	1.09	0.45	0.01	0.01	10.2	23.6	46.3	19.9
	28	500.50	0.43	0.34	77.6	17.0	4.9	0.5	0.89	0.60	0.01	0.00	10.1	30.7	55.6	3.7
L	0	495.71	0.40	0.05	83.3	15.3	1.4	0.0	0.99	0.50	0.01	0.00	9.4	26.6	55.0	8.9
	28	502.25	0.44	0.14	83.8	11.3	4.8	0.0	0.93	0.52	0.01	0.00	12.6	32.0	48.6	6.8
M	0	437.30	0.26	−0.37	73.8	10.7	15.5	0.0	1.27	0.43	0.01	0.01	2.5	11.0	53.1	33.5
	28	481.91	0.38	0.19	66.4	28.7	3.9	1.0	0.99	0.56	0.02	0.00	6.5	23.6	64.5	5.3
N*	0	486.73	0.35	−0.06	86.4	11.5	2.1	0.0	1.08	0.50	0.01	0.00	4.7	18.8	64.8	11.7
	28	494.85	0.42	0.14	87.5	9.9	2.6	0.0	0.94	0.53	0.01	0.00	11.0	28.4	55.9	4.7

Note. Sample IDs: A—*Alnus sp.*; B—*Salix sp.*; C—*Carex sp.*; D—*A. latifolia*; E—*C. rangiferina*; F—*Sphagnum sp.*; G*—charred wood; H*—charred moss; I—floodplain mud; J—active layer; K—litter layer; L—organic tundra soil; M—Yedoma permafrost; N*—charred soil. An asterisk (*) in the sample ID denotes a char sample.

NOSC = −0.08; Table 2). DOM average mass across all endmembers increased from initial composition to final, though the change was statistically insignificant (+9.14 ± 10.19 Da; $p = 0.3778$) due to the decrease in average mass exhibited by vegetation endmember samples (−12.69 ± 18.68 Da; Table 2). Considering only char, soil, and permafrost samples, average mass increased by 25.52 Da ± 10.18 Da (Table 2).

Heteroatom content remained relatively stable over the course of the biodegradation incubations, and differences in heteroatom content between pre-incubation and post-incubation DOM samples did not follow a consistent trend across endmember functional types (Figure 5). Nonetheless, several vegetation endmembers (samples A–D) and permafrost (sample M) lost a substantial RA of CHO-containing formulas accompanied by relatively high-magnitude increases in N- and/or S-containing formulas (Table 2, Figure 5b). For example, *Carex* sp. (sample C) displayed the greatest loss in CHO-formulas (−12.5%RA) with corresponding increases in CHON (7.4%RA) and CHOS (4.8%) compounds, and permafrost (sample M) presented a more minimal loss in CHO-formulas (−7.3% RA) but relatively increased in CHON-formulas by 18.0%RA (Table 2, Figure 5). There was also a distinct loss of

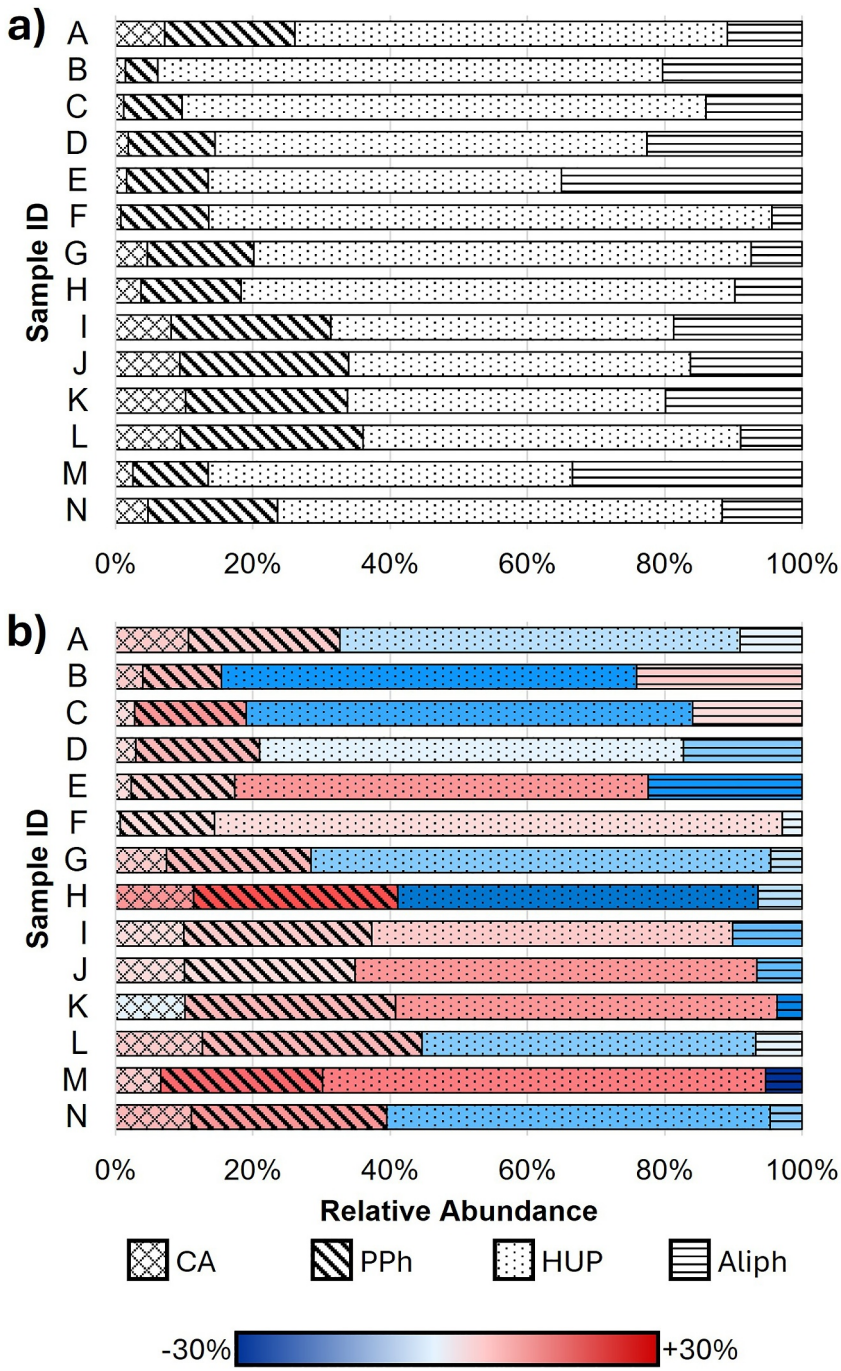

Figure 4. Endmember leachate dissolved organic matter initial ($t = 0$; panel (a)) and final ($t = 28$; panel (b)) composition by compound class. Bar patterns correspond with the different compound classes (CA = condensed aromatic, PPh = polyphenolic, HUP = highly unsaturated and phenolic, Aliph = aliphatic). Bar colors in panel (b) represent the change in relative abundance of molecular classifications from $t = 0$ to $t = 28$ (decrease in %RA = blue, increase in %RA = red). The shade of this color indicates the magnitude of change in %RA (lighter colors correspond with smaller changes while darker colors correspond to larger changes). Sample IDs: A—*Alnus sp.*; B—*Salix sp.*; C—*Carex sp.*; D—*A. latifolia*; E—*C. rangiferina*; F—*Sphagnum sp.*; G—charred wood; H—charred moss; I—floodplain mud; J—active layer; K—litter layer; L—organic tundra soil; M—Yedoma permafrost; N—charred soil.

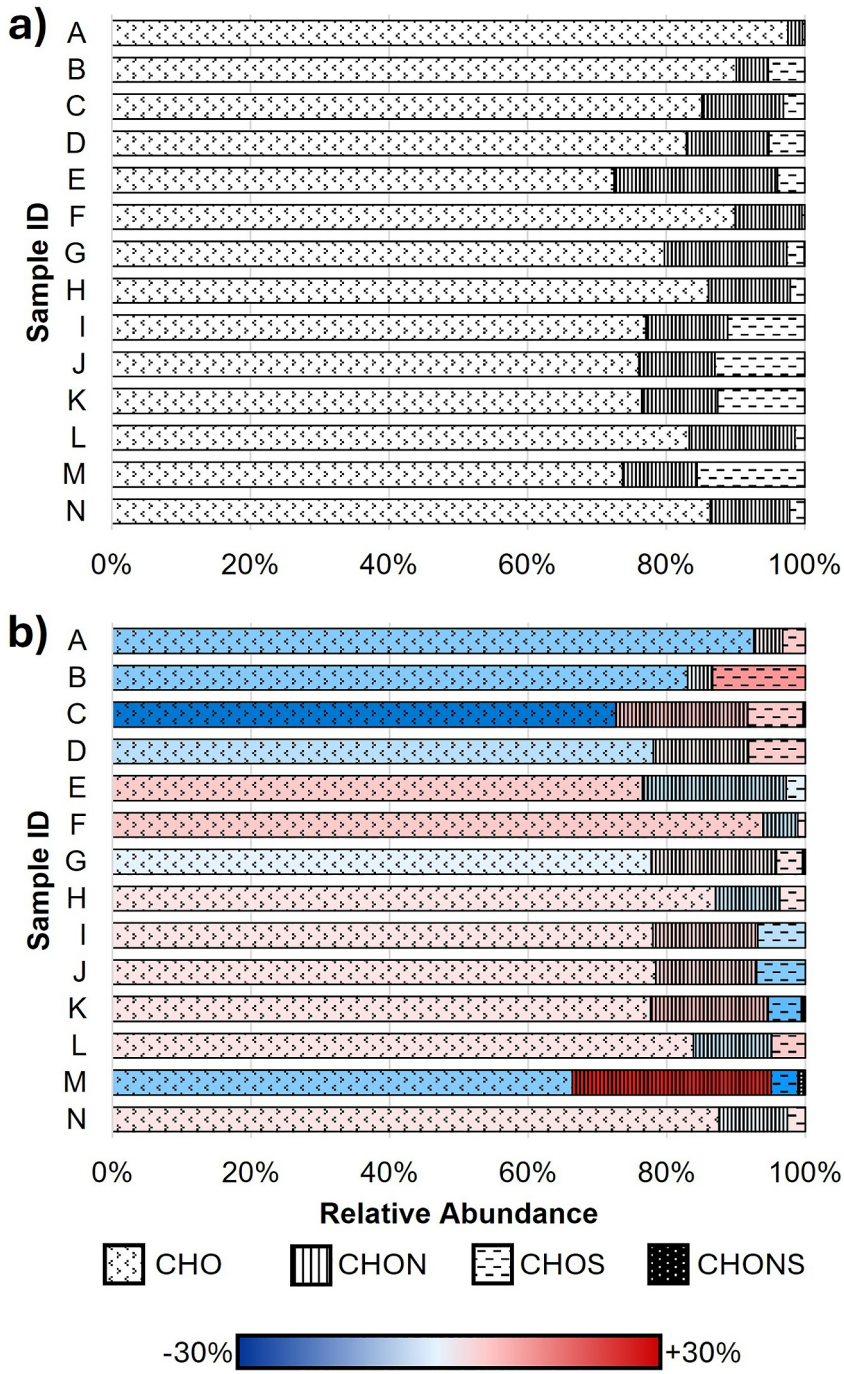

Figure 5. Endmember leachate dissolved organic matter initial ($t = 0$; panel (a)) and final ($t = 28$; panel (b)) composition by heteroatom class. Bar pattern corresponds with heteroatom class. Bar colors in panel b represent the change in relative abundance of molecular classifications from $t = 0$ to $t = 28$ (decrease in %RA = blue, increase in %RA = red). The shade of this color indicates the magnitude of change in %RA (lighter colors correspond with smaller changes while darker colors correspond to larger changes). Sample IDs: A—*Alnus sp.*; B—*Salix sp.*; C—*Carex sp.*; D—*A. latifolia*; E—*C. rangiferina*; F—*Sphagnum sp.*; G—charred wood; (H—charred moss; I—floodplain mud; J—active layer; K—litter layer; L—organic tundra soil; M—Yedoma permafrost; N—charred soil.

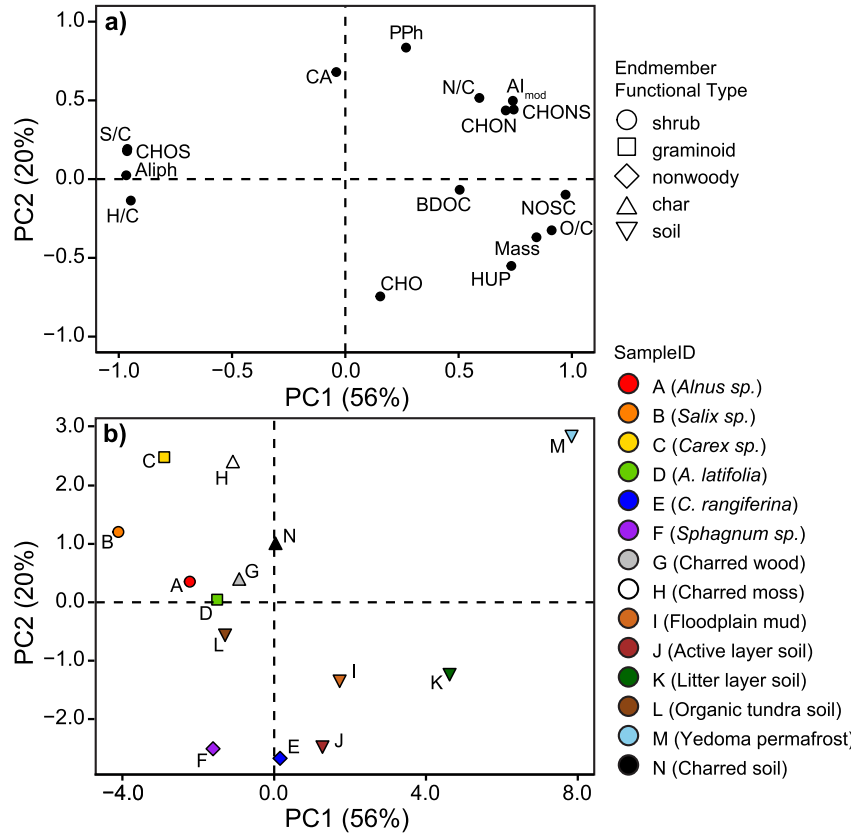

Figure 6. Principal component analysis (PCA) of %BDOC and changes in molecular-level compositional parameters before and after dissolved organic matter leachate bioincubations showing (a) the loadings for each variable and (b) the scores of each endmember leachate plotted in PCA space. Sample point shapes are grouped by endmember type and color corresponds to sample ID. CA = condensed aromatic, PPh = polyphenolic, HUP = highly unsaturated and phenolic, Aliph = aliphatic, AI_{mod} = modified aromaticity index, and NOSC = nominal oxidation state of carbon.

CHOS-formulas in mineral soils (samples I–K) and permafrost (sample M; mean −7.4 ± 3.4%RA), whereas most other samples exhibited an increase (+0.4–8.1%RA) in RA in S-containing formulas.

3.3. Drivers of Source Endmember Leachate Biodegradation

PC1 of the PC analysis described 56% of the variance between endmember leachates and is strongly positively correlated with NOSC and O/C, and negatively with H/C and aliphatics %RA, leading to a separation of samples based on endmember type (Figure 6b). For example, mineral soils (samples I, J, and K) group together in the lower right hand quadrant of the PCA shown in Figure 6b whereas shrubs and graminoids (samples A, B, C, and D) cluster in the upper left hand quadrant. Additionally, although not a major driver of the PCA, it is worth noting that a higher loss of BDOC was inversely associated with greater loss of aliphatic %RA and high-H/C formulas. PC2 explained 20% of the variance of the data set and was driven positively by changes in the %RA of CA and PPh formulas and negatively by changes in %RA of CHO-containing formulas.

4. Discussion

4.1. Ramifications of Arctic Landscape Alterations on Terrestrial Dissolved Organic Matter Mobilization

Relative contributions of soil (excluding permafrost) DOM to aquatic systems are expected to decrease significantly over the course of the 21st century, as Arctic greening (i.e., the general expansion of vegetation) has been predicted to decrease bare ground area by more than 30% by 2100 (Arens et al., 2008; Frost et al., 2024; Moon et al., 2024). As pioneer species such as *Sphagnum* and other bryophytes and nonvascular plants colonize unvegetated areas in the initial stages of vegetation succession (Mekonnen et al., 2021), the amount of DOM

exported from the terrestrial landscape via surface water flow could increase by more than one order of magnitude per our results (Table 1), effectively overprinting the signature of soil DOM in adjacent rivers with those derived from vegetation sources. In this model of succession, nonvascular plants will eventually be outcompeted by graminoids (i.e., grasses and sedges), which have been shown to initially respond well to increased temperatures in experimental setups but ultimately experience a population decline as a result of shrub proliferation (Chapin et al., 1995, 1996; Dormann & Woodin, 2002; Mod & Luoto, 2016; Wilson & Nilsson, 2009). Here, we show that mosses and lichens leach the lowest DOC concentrations of the vegetation varieties studied followed by graminoids, which on average yielded more than twice as much DOC, and finally, shrubs, which again, on average, almost doubled the DOC yields of the previous successional group (Table 1, Figure 2). Since the late-twentieth century, there has been a marked increase in the ground cover area dominated by deciduous and evergreen shrubs as well as coniferous and broadleaf trees corresponding with net decreases in area coverage by graminoids and nonvascular plants throughout Alaska (Macander et al., 2022). The Yukon River Basin includes several bioclimatic zones, all of which display similar trends in shifting dominant vegetation communities: shrubs, especially willow, alder, and birch have become increasingly abundant across the landscape over the past several decades (Tape et al., 2006), leading to widespread declines in populations of not only native tundra species, such as mosses and lichens, but graminoids and other vascular plants as well. Consequently, our results suggest each additional stage in vegetation succession toward shrub-dominated tundra via shrubification is expected to usher in significantly higher amounts of DOC being exported from the terrestrial landscape and into Arctic rivers.

Along with overall greening and shrubification of the Arctic, wildfires are likely to become a more prevalent feature of the landscape with continued climate change (McCarty et al., 2020, 2021). Even so, the ramifications of shifting wildfire regimes on DOC fluxes were less apparent than those of shifting vegetation communities in this study. Differences in DOC extracted from pyrogenic biomass compared to that of unburned, fresh biomass were inconsistent (Table 1, Figure 2); burned vegetation leached lower concentrations of DOC in comparison to fresh counterparts (i.e., *Sphagnum* moss), whereas charred soil yielded almost double the initial DOC concentration of unburned active layer tundra soil (Table 1). Despite their inconsistency, these results are well-aligned with the current literature, as the response of streams and rivers to fire have been found to be widely variable throughout the Arctic and are largely dependent on a number of factors (Betts et al., 2009; Burd et al., 2018; Parham et al., 2013; Petrone et al., 2007; Rodriguez-Cardona et al., 2020). Importantly, the extent of thermal alteration can impact several physicochemical properties of burned biomass relative to unburned biomass, including chemical composition and molecular structure (Myers-Pigg et al., 2015; Schneider et al., 2013), which further influences sorption and solubility (Wagner et al., 2017), biogeochemical reactivity, and residence time in the environment (Bird et al., 2015). For example, although low-temperature fires (below 300°C) lead to the formation of soluble and biolabile depolymerized products, high-temperature combustion (>300°C) aromatizes precursor compounds leading to increased biological stability and decreased solubility relative to the parent material (Baldock & Smernik, 2002; Knicker et al., 2008; Kuo et al., 2011). The decreased DOC yields observed in this study from charred moss leachates relative to fresh moss leachates could be a result of reduced solubility exhibited by burned biomass (Table 1; Wagner et al., 2017), which is in line with previous observations of reduced DOC mobilization from Arctic landscapes immediately after fire (e.g., Rodriguez-Cardona et al., 2020; Wei et al., 2021). The amount of time since a fire has occurred has also been shown to influence the quantity and quality of DOC exported from the landscape. Rodriguez-Cardona et al. (2020) showed that recently burned sites exhibit reduced DOC export that recovered slowly to preburn conditions over the course of approximately 50 years, whereas other studies (e.g., Wei et al., 2021) suggest a much shorter recovery time for DOC export dependent upon burn area. Char samples were collected for the present study approximately 10 months after the Apoon Pass fire took place during which time a complete freeze-thaw cycle occurred, which may have led to significant yet unidentifiable physical and compositional modifications to the char endmembers. Overall, the impacts of fire on DOC fluxes from Arctic landscapes are complex and require further refinement to determine how site conditions before (e.g., permafrost extent, vegetation cover, and community) and after (e.g., burn area, char intensity, and time passed) a fire influences the response of watershed chemistry to these disturbances.

The concentration of leachable DOC from Yedoma permafrost in this study (16.3 mg C L^{-1}; Table 1) was significantly lower than values reported by similar leaching studies (e.g., Drake, Guillemette, et al., 2018; Textor et al., 2019). However, a direct comparison of DOC yields across studies using different leaching methods is difficult especially without knowing the dry weight of the substrate (generally leached from frozen in field-moist conditions) or the total OC content of the permafrost sample. Nevertheless, DOC dissolution and mobilization

from thawing permafrost has been shown to greatly exceed carbon loss as CO_2 and CH_4 via microbial respiration in soils (Kjaer et al., 2024). Indeed, by the year 2100, thawing Yedoma permafrost throughout Siberia and Alaska is estimated to release 5.8–10.6 Tg of DOC yr^{-1}, which is equivalent to approximately a quarter of the contemporary annual DOC load exported to the Arctic Ocean from the pan-Arctic watershed (Drake, Guillemette, et al., 2018; Holmes et al., 2012). Although permafrost thaw is likely to increase DOC inputs into Arctic rivers as shown here and in the literature (Table 1; Figure 2), thawing permafrost DOM has been shown to be challenging to detect due to its rapid mineralization upon thaw further supported by our findings of high %BDOC (64.9% permafrost BDOC vs. 41.7 ± 16.5% BDOC averaged across all other endmembers; Drake et al., 2015; Spencer et al., 2015). This, in conjunction with the significantly lower DOC yields from permafrost in comparison with vegetation leachates (Table 1, Figure 2a) suggests that increased DOC inputs from thawing permafrost may have little impact on the DOC concentration or DOM composition exported to the Arctic Ocean particularly in comparison with other major landscape perturbations.

4.2. Susceptibility of Shifting Dissolved Organic Matter Sources to Biodegradation

Climate-induced landscape disturbances will alter the quality (i.e., bioavailability) of DOC mobilized from the landscape and into Arctic rivers, ultimately altering the reactivity and stability of the riverine DOM pool, as indicated by the biodegradation experiments of source endmember leachates (Figure 3). Soil organic matter was on average more bioavailable than that of vegetation-derived DOM in this study contrary to previously reported results (Pinsonneault et al., 2016; Textor et al., 2019). Vegetation and surface organic soil DOM in moss-dominated ecosystems is generally found to be more readily utilized by microbes than deeper soil horizons due to the high abundance of bioavailable chemical moieties, such as lipid-like, protein-like, and amino sugars in surface DOM (Tfaily et al., 2014, 2018). The utilization of bioavailable DOM at the surface generally leads to the accumulation of lower quality DOM at depth causing a subsequent decline in soil microbial activity (O'Donnell et al., 2016; Textor et al., 2019; Tfaily et al., 2018). Our findings suggest that greening of the Arctic landscape (i.e., colonization of the previously barren landscape with hardy pioneer species: mosses and lichens) will switch this framework reducing the bioavailability of DOC at the surface in comparison to that of soils (Table 1 and Figure 3). Further, this shift will lead to a reduction in overall bioavailability of DOC mobilized from the landscape as soil DOM fingerprints are overshadowed by higher DOC concentrations contributed by plant biomass (Table 1).

The reactivity of vegetation endmember DOC was found to be source-specific in this study, suggesting that plant community composition will also influence the quality of terrestrial DOM exported into Arctic rivers. The biodegradability of vegetation endmember leachates followed a distinct gradient: shrubs were less biodegradable than graminoids, which were less biodegradable than mosses and lichens (Figure 3). As Arctic greening, and more specifically shrubification occurs via a pathway akin to primary succession on a much larger scale (Tape et al., 2006), this distinction of DOM quality between plant functional types will have profound implications for DOM residence time via increased stability in Arctic rivers and downstream environments. The advancement of trees and shrubs into higher latitudes and altitudes has been shown to reduce the bioavailability of underlying soil DOM and disrupt microbial activity via increased polyphenolic inputs leading to the enrichment of nearby aquatic systems with biostable DOM (Catalán et al., 2024). The increased shrub abundance and patch density being observed in the Alaskan Arctic is dominated by alder (*Alnus* sp.), willow (*Salix* sp.), and dwarf birch (*Betula nana*) expansion (Sturm et al., 2001; Tape et al., 2006). Of our 14 source endmembers studied here, the alder and willow leachates (samples A and B, respectively) yielded the least bioavailable DOC of the sample set (Figure 3). Similarly, dwarf birch has been shown to be a source of highly biostable DOC when compared to native tundra vegetation types, such as lichens and sedges (Allain et al., 2024). These prolific shrubs are expected to increase their abundance in northern high-latitude and altitude by up to 35% by 2100 accompanied by a complementary decrease in nonwoody and herbaceous biomass (Macander et al., 2022; Mekonnen et al., 2018). This shift in plant community composition, which is currently dominated by mosses, grasses, and interspersed dwarf scrub species to a shrub-dominated landscape is expected to increase the stability of the DOC pool exported into Arctic rivers, thereby boosting the residence time and downstream persistence of this DOC (Catalán et al., 2024).

However, this assessment of riverine bioavailability naturally excludes processing of DOM that may occur on the landscape prior to mobilization and thus may underestimate the bioavailability of plant-derived DOC in particular. For example, decomposability of leaf litter has been linked with lignin content; increased lignin concentrations lead to decreased rates of biotic degradation (Austin & Ballaré, 2010; Bonanomi et al., 2023). Soil

microbes, white rot fungi in particular, play an integral role in lignin decomposition (Aust, 1995; Pandey & Pitman, 2003; Swift et al., 1979). Lignin content in the vegetation samples studied herein generally follows the opposite trend observed for decomposability: broadleaf plant litter contains a higher abundance of lignin than grasses and herbs, which contain more lignin than mosses and lichens, and each plant functional type contains more lignin than soils, which demonstrate decreased lignin content with depth (Chakrawal et al., 2024; Reuter et al., 2024). Although lignin content and endmember DOM biolability align with the accepted regulatory role of lignin on biomass degradation (Austin & Ballaré, 2010; Bonanomi et al., 2023; Freeman et al., 2001, 2004), the experimental assumption that plant litter DOM will be exported without modification by interactions with soil microbial communities may explain the relatively low BDOC of shrubs and graminoids as well as the discrepancy between our findings and those found in other plant and soil endmember biolability studies (i.e., that vegetation derived DOC is less bioavailable than soil DOC).

Due to the compositional complexity and heterogeneous reactivity of thermally altered organic carbon, we did not observe a discernible trend in BDOC among the charred endmembers in comparison to their unburned counterparts herein (Figure 3). Although charred moss DOC extracts exhibited greater bioavailability than unburned *Sphagnum*, burned organic soil DOC was 54% less bioavailable than unburned organic tundra soil, and charred wood had no direct unburned counterpart to compare to. Although comparisons of bioavailability between precursors and burned endmembers were limited and lacked a definitive conclusion, biodegradation experiments of charred endmembers resulted in the removal of an average of 46.2% of the total DOC, suggesting that char-derived DOM is relatively bioavailable in natural waters (Table 1). Although some fractions of thermally altered organic matter (e.g., black carbon) have been traditionally considered as largely resistant to microbial decay (Liang et al., 2008; Preston & Schmidt, 2006), this study is among several demonstrating that a significant portion of pyrogenic organic matter is readily bioavailable and stimulates microbial activity in aquatic environments (Myers-Pigg et al., 2015; Norwood et al., 2013). However, a more thorough investigation into the impacts of wildfire on DOM quality and reactivity in the changing Arctic should be conducted using a diverse host of endmembers to supplement these preliminary findings.

Permafrost DOM has consistently been observed to be highly bioavailable upon introduction into the contemporary carbon cycle, which is corroborated by the findings of this study. We found thawing Yedoma permafrost DOM to be biodegraded rapidly by Yukon River microbes, losing almost 65% of the initial DOC yield over the 28-day bottle incubations, more than half of which was degraded within the first seven days- highly comparable with past studies examining Yedoma-derived DOM bioavailability (Drake, Guillemette, et al., 2018; Holmes et al., 2008; Spencer et al., 2015; Textor et al., 2019; Vonk et al., 2013; Wickland et al., 2012). Thaw extent has been correlated with higher rates of carbon turnover via microbial respiration, demonstrating the relationship between the thaw gradient and DOC bioavailability (Hodgkins et al., 2016). The rapid utilization of permafrost DOM by riverine microbes, much of which occurs in small-order tributaries prior to confluence with major Arctic rivers (Drake et al., 2015; Spencer et al., 2015; Vonk et al., 2013), leads to an offset between the large amount of ancient DOC mobilized from the landscape via permafrost thaw and the apparent modern age of DOC exported by rivers into the Arctic Ocean (Aiken et al., 2014; Neff et al., 2006; Raymond et al., 2007; Spencer et al., 2008). The distinct lack of permafrost molecular fingerprints in this major DOM pool indicates that permafrost DOM molecular signatures do not persist into downstream environments due to rapid remineralization of bioavailable molecular formulas and compositional convergence with bulk river DOM (Drake, Guillemette, et al., 2018; Rogers et al., 2021; Spencer et al., 2015). Instead, less bioavailable DOC from modern sources, such as recently fixed plant material, will dominate the molecular signatures of DOM exported into coastal and marine environments supported by the high yields of biologically stable leachable DOC from vegetation demonstrated in this study (Table 1, Figure 2; Drake, Guillemette, et al., 2018; Spencer et al., 2015). This will lead to an overall increased resistance to microbial degradation of the downstream riverine and coastal organic matter pools, causing increased overall stability and residence time in these reservoirs and/or susceptibility to other biogeochemical processes, such as photochemical degradation (Grunert et al., 2021; Stubbins et al., 2010).

4.3. Role of Chemical Composition on the Fate of Dissolved Organic Matter

By leveraging the unparalleled mass accuracy and ultrahigh resolution of FT-ICR MS, this study showed that, regardless of endmember type, DOM degradation followed consistent trends across many molecular properties (Table 2, Figure 4). Notably, we observed a largely consistent decrease in the relative contribution of aliphatic compounds in leachate DOM following bioincubation experiments, and greater loss in aliphatic content was

correlated with greater DOC bioavailability (Figure 6). For example, permafrost DOM was highly bioavailable and rapidly utilized by Yukon River microbes; this was accompanied by a 28% loss of aliphatic %RA over the course of the biodegradation incubations (Figure 5) and overall decrease in H/C (−0.28, Table 2). It should also be noted that changes in average mass correlated with bioavailability and aliphatic %RA, whereby average mass increased following biodegradation in endmember leachates that exhibited greater BDOC and loss of aliphatic content (Table 2). This loss of high-H/C, low-MW molecular formulas, a result mirrored in several earlier studies (Allain et al., 2024; Drake et al., 2015, Drake, Guillemette, et al., 2018; Spencer et al., 2015; Textor et al., 2019), was indicative of the selective removal of these chemical moieties by riverine microbial communities. Readily assimilated low-MW aliphatic moieties such as carboxylic acids, amino acids, and carbohydrates have been shown to offer substantial support for aquatic microbial metabolism, providing up to 100% of microbial energy and carbon demand, and are in general more available to microbes than high-MW DOM (Berggren et al., 2010; Drake et al., 2015; Yang et al., 2024). Aliphatic compounds are rapidly metabolized by microbes in part due to the high energetic potential associated with low NOSC (LaRowe & Van Cappellen, 2011), an assertion strengthened by the inverse relationship between the change in aliphatic %RA and the change in NOSC over the course of the incubation experiments (Table 2, Figure 6). The preferential utilization of this high-energy subsidy as well as covariance of aliphatic content with DOC bioavailability emphasizes the apparent control of aliphatic content on microbial degradation of DOM (Figure 6).

Conversely, AI_{mod} and the RA of CA and PPh molecular formulas increased with biodegradation across all endmember leachates (Figure 6). Aromatic compounds have been shown to be preferentially preserved with soil depth and therefore degree of degradation and are also found to be more abundant in riverine DOM than in fresh source-derived allochthonous DOM (O'Donnell et al., 2016; Spencer et al., 2015; Textor et al., 2019; Tfaily et al., 2018). Moreover, the observed increase in RA of aromatic molecular formulas (Figure 4) is likely a result of the resistance of these compounds to microbial decay and thus their conservation (Drake et al., 2015; O'Donnell et al., 2016). Condensed aromatic compounds are generally the result of biomass combustion and have been shown to resist microbial decay and accumulate in carbon reservoirs over time (Wagner et al., 2021). Polyphenolic compounds, which are plant-derived secondary metabolites, are known inhibitors of microbial metabolism through the disruption of enzymatic activity in aerated and anoxic aquatic environments (Freeman et al., 2001, 2004; Mann et al., 2014). This attenuation of biological activity along with the sheer amount of energy required to break down these molecules due to electron resonance stability of aromatic rings (Fuchs et al., 2011; Harwood & Parales, 1996; LaRowe & Van Cappellen, 2011) explains the resistance to microbial degradation of PPh and CA molecular formulas shown in numerous environments and matrices (e.g., Kellerman et al., 2018). As such, the preservation of these stable compounds as well as increased inputs of aromatic molecular formulas from shrubification and shifting wildfire regimes supports the hypothesis that climate-induced landscape alterations will lead to decreased bioavailability of riverine DOM overall altering carbon export into the receiving Arctic Ocean.

4.4. Implications of Changing Terrestrial Dissolved Organic Carbon Fluxes for Downstream Environments

Our findings underscore the utility of FT-ICR MS as a tool for identifying compositional shifts associated with microbial transformation of DOM leached from different model source endmembers representative of various climate-driven landscape disturbances in the Arctic. In particular, with continued perturbations, the DOM pool exported from Arctic rivers and into coastal and marine environments will be replete of bioavailable moieties, such as aliphatic and high-H/C molecular formulas, and more abundant in oxidized and biostable molecular formulas, such as PPh and CA compounds. It has been shown that only a small portion of DOM present in seawater and/or preserved in marine sediments is terrestrially derived (Bianchi, 2011; Hedges et al., 1997), suggesting that terrestrial DOM mobilized in Arctic rivers must be mineralized, transformed, or sequestered within fluvial and coastal to marine systems.

In the Yukon River, roughly half of the total DOC exported from the river exits the plume to reach the Arctic Ocean, highlighting the importance of estuarine biogeochemical processes (Clark et al., 2022). Biodegradation processes dominate in the riverine setting and continue to be of paramount importance in estuaries (Clark et al., 2022; Grunert et al., 2021; Hedges et al., 1997). However, other processes, such as photochemical reactions (Grunert et al., 2021; Osburn et al., 2009; Stubbins et al., 2010), flocculation (Asmala et al., 2014; He et al., 2016), and adsorption processes (Groeneveld et al., 2020), begin to become more important in the coastal zone.

Photodegradation of DOC has been shown to be an important process in coastal systems globally (Osburn et al., 2009; Stubbins et al., 2010). In the Yukon River, photochemical degradation has been suggested to be responsible for the removal of only 5% of the DOC exported from the river during peak freshet (Clark et al., 2022). Photochemical reactivity in the Yukon River as well as its discharge plume is largely limited due to low light penetration caused by large amounts of suspended particulates. Nonetheless, the contribution of aromatic molecular formulas has been shown to decrease with increasing salinity from the Yukon River into the Bering Sea, emphasizing the potential importance of DOM photodegradation and/or other physicochemical transformations in Arctic estuaries (Kellerman et al., 2023). Increased flux of aromatic compounds into coastal environments from Arctic rivers may also lead to an increase in precipitation (flocculation) and subsequent sinking of organic matter, which has been shown to be an important process in the transformation of the DOM pool and removal of carbon in the coastal environment (Asmala et al., 2014; Clark et al., 2022). Terrestrially derived DOM is highly susceptible to adsorption onto inorganic particles due to its highly aromatic nature, making this a particularly important carbon sequestration process in terms of shifting terrestrial DOM sources in the Arctic (Groeneveld et al., 2020). Thus, despite the predicted evolution of the exported DOM pool toward biological stability due to climate-driven landscape alteration as highlighted by this study, there are still several carbon turnover mechanisms at play in receiving reservoirs. The potential shift in the composition of DOM mobilized from the Arctic landscape into fluvial networks as a result of climate-driven perturbations could consequently shift the importance of these other carbon cycling processes in the Yukon River plume and throughout the Arctic Ocean, not necessarily altering the rates of carbon turnover but the mechanisms by which it occurs.

5. Conclusions

Climate change and affiliated perturbations of the Arctic landscape have implications for the quantity of DOC and quality of DOM exported to and from rivers in northern high-latitude regions (Textor et al., 2019; Vonk et al., 2015). Our results provide a number of key insights with respect to the watershed response to climate-induced landscape alterations. First, shrubification and landscape greening in any capacity will drastically increase the amount and biological stability of DOM mobilized from the landscape. Second, thermally altered biomass and soil DOM properties and quality are highly dependent upon a multitude of factors, including precursor composition and extent of thermal alteration, leading to inconsistent reactivity and persistence in nature. Finally, DOC derived from thawing permafrost was found to be highly bioavailable upon introduction into the contemporary carbon cycle, which has in turn been associated with enhanced carbon turnover upon thaw in small order streams but ultimately has minimal impacts on organic carbon dynamics in larger downstream environments (Drake et al., 2015, Drake, Guillemette, et al., 2018; Spencer et al., 2015). Given the data that is currently available regarding the magnitude and extent of these climate-driven landscape disturbances, it is difficult to draw conclusions on their combined impacts on exported DOC quantities and rates of overall carbon turnover in Arctic rivers and the coastal zone. Nonetheless, our results indicate that under consistent and equal conditions, shrubification, wildfires, and permafrost thaw together would increase the concentration and biological stability of the DOC pool exported into the coastal zone via Arctic rivers. Microbial degradation of endmember leachates consistently resulted in the enrichment of aromatic molecular formulas as a result of the selective depletion of the energy-rich, bioavailable fraction of DOM, such as aliphatic and other high-H/C molecular formulas. Further, we expect a decrease in the relative importance of microbial respiration in coastal carbon turnover processes accompanied by a potential increase in the importance of photochemical and flocculation processes. Further investigation into the biological reactivity of terrestrial DOM in the coastal zone (e.g., higher salinity microbial communities) as well as its susceptibility to other carbon turnover mechanisms (e.g., photodegradation and flocculation) is needed to improve our understanding of the impacts of climate-induced landscape perturbations on carbon turnover across the land-ocean gradient.

Data Availability Statement

The authors declare that all data supporting the results of this study are archived and freely available on the Open Science Framework (Slentz, 2023; https://osf.io/qjhs9/).

Acknowledgments
The authors would like to thank Edda Mutter and the Yukon River Inter-Tribal Watershed Council for their assistance in making the fieldwork out of Alakanuk, AK possible. We acknowledge and thank our local Yup'ik collaborators for their continued support, including Augusta Edmund, Teddy Hamilton, Theo Hamilton, Sonny Isadore, and John Strongheart; without them this project would not be possible. Much of this project was conducted in the Yukon (Kuigpak) River and its coastal waters in the Yukon River National Wildlife Refuge near the villages of Alameq (Alakanuk), Imangaq (Emmonak), and Qerrulliik (Kotlik), the ancestral and current home and hunting grounds of the Yup'ik people. This work was funded by the U.S. NASA (80NSSC18K0492 and 80NSSC22K0152). A portion of this work was performed at the National High Magnetic Field Laboratory ICR User Facility, which is supported by the National Science Foundation Division of Materials Research and Division of Chemistry through DMR 16–44779 and the State of Florida.

References

Aiken, G. R., Spencer, R. G., Striegl, R. G., Schuster, P. F., & Raymond, P. A. (2014). Influences of glacier melt and permafrost thaw on the age of dissolved organic carbon in the Yukon River basin. *Global Biogeochemical Cycles*, *28*(5), 525–537. https://doi.org/10.1002/2013gb004764

Allain, A., Alexis, M. A., Bridoux, M. C., Shirokova, L. S., Payandi-Rolland, D., Pokrovsky, O. S., & Rouelle, M. (2024). The specific molecular signature of dissolved organic matter extracted from different arctic plant species persists after biodegradation. *Soil Biology and Biochemistry*, *193*, 109393. https://doi.org/10.1016/j.soilbio.2024.109393

Amon, R. M. W., Rinehart, A. J., Duan, S., Louchouarn, P., Prokushkin, A., Guggenberger, G., et al. (2012). Dissolved organic matter sources in large Arctic rivers. *Geochimica et Cosmochimica Acta*, *94*, 217–237. https://doi.org/10.1016/j.gca.2012.07.015

Arens, S. J. T., Sullivan, P. F., & Welker, J. M. (2008). Nonlinear responses to nitrogen and strong interactions with nitrogen and phosphorus additions drastically alter the structure and function of a high arctic ecosystem. *Journal of Geophysical Research*, *113*(G3), G03S09. https://doi.org/10.1029/2007jg000508

Asmala, E., Bowers, D. G., Autio, R., Kaartokallio, H., & Thomas, D. N. (2014). Qualitative changes of riverine dissolved organic matter at low salinities due to flocculation. *Journal of Geophysical Research: Biogeosciences*, *119*(10), 1919–1933. https://doi.org/10.1002/2014jg002722

Aust, S. D. (1995). Mechanisms of degradation by white rot fungi. *Environmental health perspectives*, *103*(suppl 5), 59–61. https://doi.org/10.2307/3432481

Austin, A. T., & Ballaré, C. L. (2010). Dual role of lignin in plant litter decomposition in terrestrial ecosystems. *Proceedings of the National Academy of Sciences*, *107*(10), 4618–4622. https://doi.org/10.1073/pnas.0909396107

Bahureksa, W., Borch, T., Young, R. B., Weisbrod, C., Blakney, G. T., & McKenna, A. M. (2022). Improved dynamic range, resolving power, and sensitivity achievable with FT-ICR mass spectrometry at 21 T reveals the hidden complexity of natural organic matter. *Analytical Chemistry*, *94*(32), 11382–11389. https://doi.org/10.1021/acs.analchem.2c02377

Baldock, J. A., & Smernik, R. J. (2002). Chemical composition and bioavailability of thermally altered Pinus resinosa (red pine) wood. *Organic Geochemistry*, *33*(9), 1093–1109. https://doi.org/10.1016/s0146-6380(02)00062-1

Behnke, M. I., McClelland, J. W., Tank, S. E., Kellerman, A. M., Holmes, R. M., Haghipour, N., et al. (2021). Pan-Arctic riverine dissolved organic matter: Synchronous molecular stability, shifting sources and subsidies. *Global Biogeochemical Cycles*, *35*(4), e2020GB006871. https://doi.org/10.1029/2020gb006871

Bellard, C., Bertelsmeier, C., Leadley, P., Thuiller, W., & Courchamp, F. (2012). Impacts of climate change on the future of biodiversity. *Ecology Letters*, *15*(4), 365–377. https://doi.org/10.1111/j.1461-0248.2011.01736.x

Berggren, M., Laudon, H., Haei, M., Ström, L., & Jansson, M. (2010). Efficient aquatic bacterial metabolism of dissolved low-molecular-weight compounds from terrestrial sources. *The ISME journal*, *4*(3), 408–416. https://doi.org/10.1038/ismej.2009.120

Berner, L. T., & Goetz, S. J. (2022). Satellite observations document trends consistent with a boreal forest biome shift. *Global Change Biology*, *28*(10), 3275–3292. https://doi.org/10.1111/gcb.16121

Betts, E. F., & Jones, J. B., Jr. (2009). Impact of wildfire on stream nutrient chemistry and ecosystem metabolism in boreal forest catchments of interior Alaska. *Arctic Antarctic and Alpine Research*, *41*(4), 407–417. https://doi.org/10.1657/1938-4246-41.4.407

Bianchi, T. S. (2011). The role of terrestrially derived organic carbon in the coastal ocean: A changing paradigm and the priming effect. *Proceedings of the National Academy of Sciences*, *108*(49), 19473–19481. https://doi.org/10.1073/pnas.1017982108

Bird, M. I., Wynn, J. G., Saiz, G., Wurster, C. M., & McBeath, A. (2015). The pyrogenic carbon cycle. *Annual Review of Earth and Planetary Sciences*, *43*(1), 273–298. https://doi.org/10.1146/annurev-earth-060614-105038

Blakney, G. T., Hendrickson, C. L., & Marshall, A. G. (2011). Predator data station: A fast data acquisition system for advanced FT-ICR MS experiments. *International Journal of Mass Spectrometry*, *306*(2–3), 246–252. https://doi.org/10.1016/j.ijms.2011.03.009

Bonanomi, G., Motti, R., De Marco, A., & Idbella, M. (2023). Temperature sensitivity and decomposition rate of 101 leaf litter types from mediterranean ecosystems. *Science of the Total Environment*, *894*, 165026. https://doi.org/10.1016/j.scitotenv.2023.165026

Box, J. E., Colgan, W. T., Christensen, T. R., Schmidt, N. M., Lund, M., Parmentier, F. J. W., et al. (2019). Key indicators of Arctic climate change: 1971–2017. *Environmental Research Letters*, *14*(4), 045010. https://doi.org/10.1088/1748-9326/aafc1b

Boye, K., Noël, V., Tfaily, M. M., Bone, S. E., Williams, K. H., Bargar, J. R., & Fendorf, S. (2017). Thermodynamically controlled preservation oforganic carbon in floodplains. *Nature Geoscience*, *10*(6), 415–419. https://doi.org/10.1038/ngeo2940

Burd, K., Tank, S. E., Dion, N., Quinton, W. L., Spence, C., Tanentzap, A. J., & Olefeldt, D. (2018). Seasonal shifts in export of DOC and nutrients from burned and unburned peatland-rich catchments, Northwest Territories, Canada. *Hydrology and Earth System Sciences*, *22*(8), 4455–4472. https://doi.org/10.5194/hess-22-4455-2018

Burns, A. J., Spencer, R. G. M., Kellerman, A. M., Yan, G., Leonard, L., Kaiser, K., et al. (2024). The distinct composition and transformation of terrestrial organic carbon in the Yukon River delta and plume during the mighty spring freshet. *Journal of Geophysical Research: Biogeosciences*, *129*(6), e2023JG007812. https://doi.org/10.1029/2023jg007812

Catalán, N., Rofner, C., Verpoorter, C., Pérez, M. T., Dittmar, T., Tranvik, L., et al. (2024). Treeline displacement may affect lake dissolved organic matter processing at high latitudes and altitudes. *Nature Communications*, *15*(1), 2640. https://doi.org/10.1038/s41467-024-46789-5

Chakrawal, A., Lindahl, B. D., Qafoku, O., & Manzoni, S. (2024). Comparing plant litter molecular diversity assessed from proximate analysis and 13C NMR spectroscopy. *Soil Biology and Biochemistry*, *197*, 109517. https://doi.org/10.1016/j.soilbio.2024.109517

Chapin, F. S., III, & Shaver, G. R. (1996). Physiological and growth responses of arctic plants to a field experiment simulating climatic change. *Ecology*, *77*(3), 822–840. https://doi.org/10.2307/2265504

Chapin, F. S., III, Shaver, G. R., Giblin, A. E., Nadelhoffer, K. J., & Laundre, J. A. (1995). Responses of arctic tundra to experimental and observed changes in climate. *Ecology*, *76*(3), 694–711. https://doi.org/10.2307/1939337

Clark, J. B., Mannino, A., Tzortziou, M., Spencer, R. G., & Hernes, P. (2022). The transformation and export of organic carbon across an arctic river-delta-ocean continuum. *Journal of Geophysical Research: Biogeosciences*, *127*(12), e2022JG007139. https://doi.org/10.1029/2022jg007139

Corilo, Y. E. (2014). *PetroOrg software*. Florida State University. Omics LLC: Tallahassee, Fl.

D'Andrilli, J., Cooper, W. T., Foreman, C. M., & Marshall, A. G. (2015). An ultrahigh-resolution mass spectrometry index to estimate natural organic matter lability. *Rapid Communications in Mass Spectrometry*, *29*(24), 2385–2401. https://doi.org/10.1002/rcm.7400

Dittmar, T., Koch, B., Hertkorn, N., & Kattner, G. (2008). A simple and efficient method for the solid-phase extraction of dissolved organic matter (SPE-DOM) from seawater. *Limnology and Oceanography: Methods*, *6*(6), 230–235. https://doi.org/10.4319/lom.2008.6.230

Dormann, C. F., & Woodin, S. J. (2002). Climate change in the Arctic: Using plant functional types in a meta-analysis of field experiments. *Functional Ecology*, *16*(1), 4–17. https://doi.org/10.1046/j.0269-8463.2001.00596.x

Drake, T. W., Guillemette, F., Hemingway, J. D., Chanton, J. P., Podgorski, D. C., Zimov, N. S., & Spencer, R. G. (2018). The ephemeral signature of permafrost carbon in an Arctic fluvial network. *Journal of Geophysical Research: Biogeosciences*, *123*(5), 1475–1485. https://doi.org/10.1029/2017jg004311

Drake, T. W., Tank, S. E., Zhulidov, A. V., Holmes, R. M., Gurtovaya, T., & Spencer, R. G. (2018). Increasing alkalinity export from large Russian Arctic rivers. *Environmental Science and Technology*, *52*(15), 8302–8308. https://doi.org/10.1021/acs.est.8b01051

Drake, T. W., Wickland, K. P., Spencer, R. G., McKnight, D. M., & Striegl, R. G. (2015). Ancient low–molecular-weight organic acids in permafrost fuel rapid carbon dioxide production upon thaw. *Proceedings of the National Academy of Sciences*, *112*(45), 13946–13951. https://doi.org/10.1073/pnas.1511705112

Elmendorf, S. C., Henry, G. H., Hollister, R. D., Björk, R. G., Boulanger-Lapointe, N., Cooper, E. J., et al. (2012). Plot-scale evidence of tundra vegetation change and links to recent summer warming. *Nature Climate Change*, *2*(6), 453–457. https://doi.org/10.1038/nclimate1465

Emmett, M. R., White, F. M., Hendrickson, C. L., Shi, S. D.-H., & Marshall, A. G. (1998). Application of micro-electrospray liquid chromatography techniques to FT-ICR MS to enable high-sensitivity biological analysis. *Journal of the American Society for Mass Spectrometry*, *9*(4), 333–340. https://doi.org/10.1016/s1044-0305(97)00287-0

Freeman, C., Ostle, N., & Kang, H. (2001). A shortage of oxygen locks up carbon in peatlands by restraining a single enzyme. *Nature*, *409*(6817), 149–150. https://doi.org/10.1038/35051650

Freeman, C., Ostle, N. J., Fenner, N., & Kang, H. (2004). A regulatory role for phenol oxidase during decomposition in peatlands. *Soil Biology and Biochemistry*, *36*(10), 1663–1667. https://doi.org/10.1016/j.soilbio.2004.07.012

Frost, G. V., Bhatt, U., Macander, M., Berner, L. T., Bartsch, A., Bjerke, J. W., et al. (2024). The changing face of the Arctic: Four decades of greening and implications for Tundra ecosystems. *Frontiers in Environmental Science*, *13*, 1525574. https://doi.org/10.3389/fenvs.2025.1525574

Fuchs, G., Boll, M., & Heider, J. (2011). Microbial degradation of aromatic compounds—from one strategy to four. *Nature Reviews Microbiology*, *9*(11), 803–816. https://doi.org/10.1038/nrmicro2652

Groeneveld, M., Catalán, N., Attermeyer, K., Hawkes, J., Einarsdóttir, K., Kothawala, D., et al. (2020). Selective adsorption of terrestrial dissolved organic matter to inorganic surfaces along a boreal inland water continuum. *Journal of Geophysical Research: Biogeosciences*, *125*(3), e2019JG005236. https://doi.org/10.1029/2019jg005236

Grunert, B. K., Tzortziou, M., Neale, P., Menendez, A., & Hernes, P. (2021). DOM degradation by light and microbes along the Yukon River-coastal ocean continuum. *Scientific Reports*, *11*(1), 10236. https://doi.org/10.1038/s41598-021-89327-9

Harwood, C. S., & Parales, R. E. (1996). The β-ketoadipate pathway and the biology of self-identity. *Annual Review of Microbiology*, *50*(1), 553–590. https://doi.org/10.1146/annurev.micro.50.1.553

He, W., Chen, M., Schlautman, M. A., & Hur, J. (2016). Dynamic exchanges between DOM and POM pools in coastal and inland aquatic ecosystems: A review. *Science of the Total Environment*, *551*, 415–428. https://doi.org/10.1016/j.scitotenv.2016.02.031

Hedges, J. I., Keil, R. G., & Benner, R. (1997). What happens to terrestrial organic matter in the ocean? *Organic Geochemistry*, *27*(5–6), 195–212. https://doi.org/10.1016/s0146-6380(97)00066-1

Hendrickson, C. L., Quinn, J. P., Kaiser, N. K., Smith, D. F., Blakney, G. T., Chen, T., et al. (2015). 21 Tesla Fourier transform ion cyclotron resonance mass spectrometer: A national resource for ultrahigh resolution mass analysis. *Journal of the American Society for Mass Spectrometry*, *26*(9), 1626–1632. https://doi.org/10.1007/s13361-015-1182-2

Hernes, P. J., Spencer, R. G., Dyda, R. Y., O'Geen, A. T., & Dahlgren, R. A. (2017). The genesis and exodus of vascular plant DOM from an oak woodland landscape. *Frontiers in Earth Science*, *5*, 9. https://doi.org/10.3389/feart.2017.00009

Hodgkins, S. B., Tfaily, M. M., Podgorski, D. C., McCalley, C. K., Saleska, S. R., Crill, P. M., et al. (2016). Elemental composition and optical properties reveal changes in dissolved organic matter along a permafrost thaw chronosequence in a subarctic peatland. *Geochimica et Cosmochimica Acta*, *187*, 123–140. https://doi.org/10.1016/j.gca.2016.05.015

Holmes, R. M., Coe, M. T., Fiske, G. J., Gurtovaya, T., McClelland, J. W., Shiklomanov, A. I., et al. (2013). Climate change impacts on the hydrology and biogeochemistry of Arctic rivers. *Climatic change and global warming of inland waters*, 1–26. https://doi.org/10.1002/9781118470596.ch1

Holmes, R. M., McClelland, J. W., Peterson, B. J., Tank, S. E., Bulygina, E., Eglinton, T. I., et al. (2012). Seasonal and annual fluxes of nutrients and organic matter from large rivers to the Arctic Ocean and surrounding seas. *Estuaries and Coasts*, *35*(2), 369–382. https://doi.org/10.1007/s12237-011-9386-6

Holmes, R. M., McClelland, J. W., Raymond, P. A., Frazer, B. B., Peterson, B. J., & Stieglitz, M. (2008). Lability of DOC transported by Alaskan rivers to the Arctic Ocean. *Geophysical Research Letters*, *35*(3), L03402. https://doi.org/10.1029/2007gl032837

Hughey, C. A., Hendrickson, C. L., Rodgers, R. P., Marshall, A. G., & Qian, K. (2001). Kendrick mass defect spectroscopy: A compact visual analysis for ultrahigh-resolution Broadband mass Spectra. *Analytical Chemistry*, *73*(19), 4676–4681. https://doi.org/10.1021/ac010560w

Johnston, S. E., Bogard, M. J., Rogers, J. A., Butman, D., Striegl, R. G., Dornblaser, M., & Spencer, R. G. (2019). Constraining dissolved organic matter sources and temporal variability in a sub-Arctic lake. *Biogeochemistry*, *146*(3), 271–292. https://doi.org/10.1007/s10533-019-00619-9

Johnston, S. E., Shorina, N., Bulygina, E., Vorobjeva, T., Chupakova, A., Klimov, S. I., et al. (2018). Flux and seasonality of dissolved organic matter from the Northern Dvina (Severnaya Dvina) River, Russia. *Journal of Geophysical Research: Biogeosciences*, *123*(3), 1041–1056. https://doi.org/10.1002/2017jg004337

Kellerman, A. M., Dittmar, T., Kothawala, D. N., & Tranvik, L. J. (2014). Chemodiversity of dissolved organic matter in lakes driven by climate and hydrology. *Nature Communications*, *5*(1), 3804. https://doi.org/10.1038/ncomms4804

Kellerman, A. M., Guillemette, F., Podgorski, D. C., Aiken, G. R., Butler, K. D., & Spencer, R. G. M. (2018). Unifying concepts linking dissolved organic matter composition to persistence in aquatic ecosystems. *Environmental Science and Technology*, *11*.

Kellerman, A. M., Hernes, P. J., McKenna, A. M., Clark, J. B., Edmund, A., Grunert, B., et al. (2023). Mixing behavior of dissolved organic matter at the Yukon and Kolyma land ocean interface. *Marine Chemistry*, *255*, 104281. https://doi.org/10.1016/j.marchem.2023.104281

Kellerman, A. M., Kothawala, D. N., Dittmar, T., & Tranvik, L. J. (2015). Persistence of dissolved organic matter in lakes related to its molecular characteristics. *Nature Geoscience*, *8*(6), 454–457. https://doi.org/10.1038/ngeo2440

Kendrick, E. (1963). A mass scale based on CH_2 = 14.0000 for high resolution mass spectrometry of organic compounds. *Analytical Chemistry*, *35*(13), 2146–2154. https://doi.org/10.1021/ac60206a048

Kharuk, V. I., Dvinskaya, M. L., Im, S. T., Golyukov, A. S., & Smith, K. T. (2022). Wildfires in the Siberian arctic. *Fire*, *5*(4), 106. https://doi.org/10.3390/fire5040106

Kim, S., Kramer, R. W., & Hatcher, P. G. (2003). Graphical method for analysis of ultrahigh-resolution Broadband Mass Spectra of natural organic matter, the Van Krevelen diagram. *Analytical Chemistry*, *75*(20), 5336–5344. https://doi.org/10.1021/ac034415p

Kjaer, S. T., Westermann, S., Nedkvitne, N., & Dörsch, P. (2024). Carbon degradation and mobilisation potentials of thawing permafrost peatlands in northern Norway inferred from laboratory incubations. *Biogeosciences*, *21*(21), 4723–4737. https://doi.org/10.5194/bg-21-4723-2024

Knicker, H., Hilscher, A., González-Vila, F. J., & Almendros, G. (2008). A new conceptual model for the structural properties of char produced during vegetation fires. *Organic Geochemistry*, *39*(8), 935–939. https://doi.org/10.1016/j.orggeochem.2008.03.021

Koch, B. P., & Dittmar, T. (2016). From mass to structure: An aromaticity index for high-resolution mass data of natural organic matter. *RapidCommunications in Mass Spectrometry*, *30*(1), 250. https://doi.org/10.1002/rcm.7433

Koch, B. P., & Dittmar, T. (2006). From mass to structure: An aromaticity index for high-resolution mass data of natural organic matter. *RapidCommunications in Mass Spectrometry*, *20*(5), 926–932. https://doi.org/10.1002/rcm.2386

Kuo, L. J., Louchouarn, P., & Herbert, B. E. (2011). Influence of combustion conditions on yields of solvent-extractable anhydrosugars and lignin phenols in chars: Implications for characterizations of biomass combustion residues. *Chemosphere*, *85*(5), 797–805. https://doi.org/10.1016/j.chemosphere.2011.06.074

Kurek, M. R., Frey, K. E., Guillemette, F., Podgorski, D. C., Townsend-Small, A., Arp, C. D., et al. (2022). Trapped under ice: Spatial and seasonal dynamics of dissolved organic matter composition in tundra lakes. *Journal of Geophysical Research: Biogeosciences*, *127*(4), e2021JG006578. https://doi.org/10.1029/2021jg006578

LaRowe, D. E., & Van Cappellen, P. (2011). Degradation of natural organic matter: A thermodynamic analysis. *Geochimica et Cosmochimica Acta*, *75*(8), 2030–2042. https://doi.org/10.1016/j.gca.2011.01.020

Lawrence, D. M., Slater, A. G., & Swenson, S. C. (2012). Simulation of present-day and future permafrost and seasonally frozen ground conditions in CCSM4. *Journal of Climate*, *25*(7), 2207–2225. https://doi.org/10.1175/jcli-d-11-00334.1

Lê, S., Josse, J., & Husson, F. (2008). FactoMineR: An R package for multivariate analysis. *Journal of Statistical Software*, *25*(1), 1–18. https://doi.org/10.18637/jss.v025.i01

Liang, B., Lehmann, J., Solomon, D., Sohi, S., Thies, J. E., Skjemstad, J. O., et al. (2008). Stability of biomass-derived black carbon in soils. *Geochimica et Cosmochimica Acta*, *72*(24), 6069–6078. https://doi.org/10.1016/j.gca.2008.09.028

Macander, M. J., Nelson, P. R., Nawrocki, T. W., Frost, G. V., Orndahl, K. M., Palm, E. C., et al. (2022). Time-series maps reveal widespread change in plant functional type cover across Arctic and boreal Alaska and Yukon. *Environmental Research Letters*, *17*(5), 054042. https://doi.org/10.1088/1748-9326/ac6965

Mann, P. J., Sobczak, W. V., LaRue, M. M., Bulygina, E., Davydova, A., Vonk, J. E., et al. (2014). Evidence for key enzymatic controls on metabolism of Arctic River organic matter. *Global Change Biology*, *20*(4), 1086–1100. https://doi.org/10.1111/gcb.12416

McCarty, J. L., Aalto, J., Paunu, V. V., Arnold, S. R., Eckhardt, S., Klimont, Z., & Wilson, S. (2021). Reviews and syntheses: Arctic fire regimes and emissions in the 21st century. *Biogeosciences Discussions*, *2021*, 1–59.

McCarty, J. L., Smith, T. E., & Turetsky, M. R. (2020). Arctic fires re-emerging. *Nature Geoscience*, *13*(10), 658–660. https://doi.org/10.1038/s41561-020-00645-5

McClelland, J. W., Holmes, R. M., Dunton, K. H., & Macdonald, R. W. (2012). The Arctic ocean estuary. *Estuaries and Coasts*, *35*(2), 353–368. https://doi.org/10.1007/s12237-010-9357-3

Mekonnen, Z. A., Riley, W. J., Berner, L. T., Bouskill, N. J., Torn, M. S., Iwahana, G., et al. (2021). Arctic tundra shrubification: A review of mechanisms and impacts on ecosystem carbon balance. *Environmental Research Letters*, *16*(5), 053001. https://doi.org/10.1088/1748-9326/abf28b

Mekonnen, Z. A., Riley, W. J., & Grant, R. F. (2018). 21st century tundra shrubification could enhance net carbon uptake of North America Arctic tundra under an RCP8. 5 climate trajectory. *Environmental Research Letters*, *13*(5), 054029. https://doi.org/10.1088/1748-9326/aabf28

Meredith, M., Sommerkorn, M., Cassotta, S., Derksen, C., Ekaykin, A., Hollowed, A., et al. (2019). Polar regions. In *IPCC Special Report on the Ocean and Cryosphere in a Changing Climate* (pp. 203–320). Cambridge University Press.

Miner, K. R., Turetsky, M. R., Malina, E., Bartsch, A., Tamminen, J., McGuire, A. D., et al. (2022). Permafrost carbon emissions in a changing Arctic. *Nature Reviews Earth and Environment*, *3*(1), 55–67. https://doi.org/10.1038/s43017-021-00230-3

Mod, H. K., & Luoto, M. (2016). Arctic shrubification mediates the impacts of warming climate on changes to tundra vegetation. *Environmental Research Letters*, *11*(12), 124028. https://doi.org/10.1088/1748-9326/11/12/124028

Moon, T. A., Druckenmiller, M. L., & Thoman, R. L. (2024). Arctic Report Card 2024.

Myers-Pigg, A. N., Louchouarn, P., Amon, R. M., Prokushkin, A., Pierce, K., & Rubtsov, A. (2015). Labile pyrogenic dissolved organic carbon in major Siberian Arctic rivers: Implications for wildfire-stream metabolic linkages. *Geophysical Research Letters*, *42*(2), 377–385. https://doi.org/10.1002/2014gl062762

Natali, S. M., Rogers, B., Schuur, E. A., Romanovsky, V., Alcock, H., Arndt, K., et al. (2024). NOAA Arctic report card 2024: Arctic terrestrial carbon cycling.

Natali, S. M., Schuur, E. A., Webb, E. E., Pries, C. E. H., & Crummer, K. G. (2014). Permafrost degradation stimulates carbon loss from experimentally warmed tundra. *Ecology*, *95*(3), 602–608. https://doi.org/10.1890/13-0602.1

Natali, S. M., Schuur, E. A. G., & Rubin, R. L. (2012). Increased plant productivity in Alaskan tundra as a result of experimental warming of soil and permafrost. *Journal of Ecology*, *100*(2), 488–498. https://doi.org/10.1111/j.1365-2745.2011.01925.x

Neff, J. C., Finlay, J. C., Zimov, S. A., Davydov, S. P., Carrasco, J. J., Schuur, E. A. G., & Davydova, A. I. (2006). Seasonal changes in the age and structure of dissolved organic carbon in Siberian rivers and streams. *Geophysical Research Letters*, *33*(23), L23401. https://doi.org/10.1029/2006gl028222

Norwood, M. J., Louchouarn, P., Kuo, L. J., & Harvey, O. R. (2013). Characterization and biodegradation of water-soluble biomarkers and organic carbon extracted from low temperature chars. *Organic Geochemistry*, *56*, 111–119. https://doi.org/10.1016/j.orggeochem.2012.12.008

O'Donnell, J. A., Aiken, G. R., Butler, K. D., Guillemette, F., Podgorski, D. C., & Spencer, R. G. (2016). DOM composition and transformation in boreal forest soils: The effects of temperature and organic-horizon decomposition state. *Journal of Geophysical Research: Biogeosciences*, *121*(10), 2727–2744. https://doi.org/10.1002/2016jg003431

O'Donnell, J. A., Aiken, G. R., Kane, E. S., & Jones, J. B. (2010). Source water controls on the character and origin of dissolved organic matter in streams of the Yukon River basin, Alaska. *Journal of Geophysical Research*, *115*(G3), G03025. https://doi.org/10.1029/2009jg001153

Osburn, C. L., Retamal, L., & Vincent, W. F. (2009). Photoreactivity of chromophoric dissolved organic matter transported by the Mackenzie River to the Beaufort Sea. *Marine Chemistry*, *115*(1–2), 10–20. https://doi.org/10.1016/j.marchem.2009.05.003

Pandey, K. K., & Pitman, A. J. (2003). FTIR studies of the changes in wood chemistry following decay by brown-rot and white-rot fungi. *International Biodeterioration & Biodegradation*, *52*(3), 151–160. https://doi.org/10.1016/s0964-8305(03)00052-0

Parham, L. M., Prokushkin, A. S., Pokrovsky, O. S., Titov, S. V., Grekova, E., Shirokova, L. S., & McDowell, W. H. (2013). Permafrost and fire as regulators of stream chemistry in basins of the Central Siberian Plateau. *Biogeochemistry*, *116*(1–3), 55–68. https://doi.org/10.1007/s10533-013-9922-5

Petrone, K. C., Hinzman, L. D., Shibata, H., Jones, J. B., & Boone, R. D. (2007). The influence of fire and permafrost on sub-arctic stream chemistry during storms. *Hydrological Processes: International Journal*, *21*(4), 423–434. https://doi.org/10.1002/hyp.6247

Pinsonneault, A. J., Moore, T. R., Roulet, N. T., & Lapierre, J. F. (2016). Biodegradability of vegetation-derived dissolved organic carbon in a cool temperate ombrotrophic bog. *Ecosystems*, *19*(6), 1023–1036. https://doi.org/10.1007/s10021-016-9984-z

Preston, C. M., & Schmidt, M. W. (2006). Black (pyrogenic) carbon: A synthesis of current knowledge and uncertainties with special consideration of boreal regions. *Biogeosciences*, *3*(4), 397–420. https://doi.org/10.5194/bg-3-397-2006

Rantanen, M., Karpechko, A. Y., Lipponen, A., Nordling, K., Hyvärinen, O., Ruosteenoja, K., et al. (2022). The Arctic has warmed nearly four times faster than the globe since 1979. *Communications Earth & Environment*, *3*(1), 168. https://doi.org/10.1038/s43247-022-00498-3

Raymond, P. A., McClelland, J. W., Holmes, R. M., Zhulidov, A. V., Mull, K., Peterson, B. J., et al. (2007). Flux and age of dissolved organic carbon exported to the Arctic Ocean: A carbon isotopic study of the five largest arctic rivers. *Global Biogeochemical Cycles*, *21*(4), GB4011. https://doi.org/10.1029/2007gb002934

Rees, W. G., Hofgaard, A., Boudreau, S., Cairns, D. M., Harper, K., Mamet, S., et al. (2020). Is subarctic forest advance able to keep pace with climate change? *Global Change Biology*, *26*(7), 3965–3977. https://doi.org/10.1111/gcb.15113

Reuter, J., Reuter, H., & Zak, D. (2024). Decomposition of lignin and carbohydrates in a rewetted peatland: A comparative analysis of surface water and anaerobic soil layers. *Biogeochemistry*, *167*(4), 545–561. https://doi.org/10.1007/s10533-023-01102-2

Rodriguez-Cardona, B. M., Coble, A. A., Wymore, A. S., Kolosov, R., Podgorski, D. C., Zito, P., et al. (2020). Wildfires lead to decreased carbon and increased nitrogen concentrations in upland arctic streams. *Scientific Reports*, *10*(1), 8722. https://doi.org/10.1038/s41598-020-65520-0

Rogers, J. A., Galy, V., Kellerman, A. M., Chanton, J. P., Zimov, N., & Spencer, R. G. (2021). Limited presence of permafrost dissolved organic matter in the Kolyma River, Siberia revealed by ramped oxidation. *Journal of Geophysical Research: Biogeosciences*, *126*(7), e2020JG005977. https://doi.org/10.1029/2020jg005977

Šantl-Temkiv, T., Finster, K., Dittmar, T., Hansen, B. M., Thyrhaug, R., Nielsen, N. W., & Karlson, U. G. (2013). Hailstones: A window into themicrobial and chemical inventory of a storm cloud. *PLoS One*, *8*(1), e53550. https://doi.org/10.1371/journal.pone.0053550

Savory, J. J., Kaiser, N. K., McKenna, A. M., Xian, F., Blakney, G. T., Rodgers, R. P., et al. (2011). Parts-Per-Billion Fourier transform ion cyclotron resonance mass measurement accuracy with a "Walking" calibration equation. *Analytical Chemistry*, *83*(5), 1732–1736. https://doi.org/10.1021/ac102943z

Schneider, M. P., Pyle, L. A., Clark, K. L., Hockaday, W. C., Masiello, C. A., & Schmidt, M. W. (2013). Toward a "molecular thermometer" to estimate the charring temperature of wildland charcoals derived from different biomass sources. *Environmental Science and Technology*, *47*(20), 11490–11495. https://doi.org/10.1021/es401430f

Schuur, E. A., Bockheim, J., Canadell, J. G., Euskirchen, E., Field, C. B., Goryachkin, S. V., et al. (2008). Vulnerability of permafrost carbon to climate change: Implications for the global carbon cycle. *BioScience*, *58*(8), 701–714. https://doi.org/10.1641/b580807

Schuur, E. A., McGuire, A. D., Schädel, C., Grosse, G., Harden, J. W., Hayes, D. J., et al. (2015). Climate change and the permafrost carbon feedback. *Nature*, *520*(7546), 171–179. https://doi.org/10.1038/nature14338

Slentz, A. E. (2023). Terrigenous dissolved organic matter in the Yukon River Delta [Dataset]. *OSF*. https://doi.org/10.17605/OSF.IO/QJHS9

Smith, D. F., Podgorski, D. C., Rodgers, R. P., Blakney, G. T., & Hendrickson, C. L. (2018). 21 Tesla FT-ICR mass spectrometer for ultrhigh resolution analysis of complex organic mixtures. *Analytical Chemistry*, *90*(3), 2041–2047. https://doi.org/10.1021/acs.analchem.7b04159

Spencer, R. G., Aiken, G. R., Wickland, K. P., Striegl, R. G., & Hernes, P. J. (2008). Seasonal and spatial variability in dissolved organic matter quantity and composition from the Yukon River basin, Alaska. *Global Biogeochemical Cycles*, *22*(4), GB4002. https://doi.org/10.1029/2008gb003231

Spencer, R. G., Mann, P. J., Dittmar, T., Eglinton, T. I., McIntyre, C., Holmes, R. M., et al. (2015). Detecting the signature of permafrost thaw in Arctic rivers. *Geophysical Research Letters*, *42*(8), 2830–2835. https://doi.org/10.1002/2015gl063498

Starr, S., Johnston, S. E., Sobolev, N., Perminova, I., Kellerman, A., Fiske, G., et al. (2023). Characterizing uncertainty in Pan-Arctic land-ocean dissolved organic carbon flux: Insights from the Onega River, Russia. *Journal of Geophysical Research: Biogeosciences*, *128*(5), e2022JG007073. https://doi.org/10.1029/2022jg007073

Strauss, J., Laboor, S., Schirrmeister, L., Fedorov, A. N., Fortier, D., Froese, D., et al. (2021). Circum-Arctic map of the Yedoma permafrost domain. *Frontiers in Earth Science*, *9*, 758360. https://doi.org/10.3389/feart.2021.758360

Stubbins, A., & Dittmar, T. (2012). Low volume quantification of dissolved organic carbon and dissolved nitrogen. *Limnology and Oceanography: Methods*, *10*(5), 347–352. https://doi.org/10.4319/lom.2012.10.347

Stubbins, A., Spencer, R. G., Chen, H., Hatcher, P. G., Mopper, K., Hernes, P. J., et al. (2010). Illuminated darkness: Molecular signatures of Congo River dissolved organic matter and its photochemical alteration as revealed by ultrahigh precision mass spectrometry. *Limnology & Oceanography*, *55*(4), 1467–1477. https://doi.org/10.4319/lo.2010.55.4.1467

Sturm, M., Racine, C., & Tape, K. (2001). Increasing shrub abundance in the Arctic. *Nature*, *411*(6837), 546–547. https://doi.org/10.1038/35079180

Swift, M. J., Heal, O. W., Anderson, J. M., & Anderson, J. M. (1979). *Decomposition in terrestrial ecosystems* (Vol. 5). University of California Press.

Tank, S. E., McClelland, J. W., Spencer, R. G., Shiklomanov, A. I., Suslova, A., Moatar, F., et al. (2023). Recent trends in the chemistry of major northern rivers signal widespread Arctic change. *Nature Geoscience*, *16*(9), 789–796. https://doi.org/10.1038/s41561-023-01247-7

Tape, K. E. N., Sturm, M., & Racine, C. (2006). The evidence for shrub expansion in Northern Alaska and the Pan-Arctic. *Global Change Biology*, *12*(4), 686–702. https://doi.org/10.1111/j.1365-2486.2006.01128.x

Textor, S. R., Wickland, K. P., Podgorski, D. C., Johnston, S. E., & Spencer, R. G. (2019). Dissolved organic carbon turnover in permafrost-influenced watersheds of interior Alaska: Molecular insights and the priming effect. *Frontiers in Earth Science*, *7*, 275. https://doi.org/10.3389/feart.2019.00275

Tfaily, M. M., Cooper, W. T., Kostka, J. E., Chanton, P. R., Schadt, C. W., Hanson, P. J., et al. (2014). Organic matter transformation in the peat column at Marcell Experimental Forest: Humification and vertical stratification. *Journal of Geophysical Research: Biogeosciences*, *119*(4), 661–675. https://doi.org/10.1002/2013jg002492

Tfaily, M. M., Wilson, R. M., Cooper, W. T., Kostka, J. E., Hanson, P., & Chanton, J. P. (2018). Vertical stratification of peat pore water dissolved organic matter composition in a peat bog in northern Minnesota. *Journal of Geophysical Research: Biogeosciences*, *123*(2), 479–494. https://doi.org/10.1002/2017jg004007

Tranvik, L. J., Downing, J. A., Cotner, J. B., Loiselle, S. A., Striegl, R. G., Ballatore, T. J., et al. (2009). Lakes and reservoirs as regulators of carbon cycling and climate. *Limnology & Oceanography*, *54*(6part2), 2298–2314. https://doi.org/10.4319/lo.2009.54.6_part_2.2298

Veraverbeke, S., Delcourt, C. J., Kukavskaya, E., Mack, M., Walker, X., Hessilt, T., et al. (2021). Direct and longer-term carbon emissions from arctic-boreal fires: A short review of recent advances. *Current Opinion in Environmental Science & Health*, *23*, 100277. https://doi.org/10.1016/j.coesh.2021.100277

Vonk, J. E., Mann, P. J., Davydov, S., Davydova, A., Spencer, R. G., Schade, J., et al. (2013). High biolability of ancient permafrost carbon upon thaw. *Geophysical Research Letters*, *40*(11), 2689–2693. https://doi.org/10.1002/grl.50348

Vonk, J. E., Tank, S. E., Mann, P. J., Spencer, R. G., Treat, C. C., Striegl, R. G., et al. (2015). Biodegradability of dissolved organic carbon in permafrost soils and aquatic systems: A meta-analysis. *Biogeosciences*, *12*(23), 6915–6930. https://doi.org/10.5194/bg-12-6915-2015

Wagner, S., Coppola, A. I., Stubbins, A., Dittmar, T., Niggemann, J., Drake, T. W., et al. (2021). Questions remain about the biolability of dissolved black carbon along the combustion continuum. *Nature Communications*, *12*(1), 4281. https://doi.org/10.1038/s41467-021-24477-y

Wagner, S., Ding, Y., & Jaffé, R. (2017). A new perspective on the apparent solubility of dissolved black carbon. *Frontiers in Earth Science*, *5*, 75. https://doi.org/10.3389/feart.2017.00075

Wei, X., Hayes, D. J., & Fernandez, I. (2021). Fire reduces riverine DOC concentration draining a watershed and alters post-fire DOC recovery patterns. *Environmental Research Letters*, *16*(2), 024022. https://doi.org/10.1088/1748-9326/abd7ae

Wickham, H. (2016). Programming with ggplot2. In *Ggplot2: Elegant graphics for data analysis* (pp. 241–253). Springer International Publishing.

Wickland, K. P., Aiken, G. R., Butler, K., Dornblaser, M. M., Spencer, R. G. M., & Striegl, R. G. (2012). Biodegradability of dissolved organic carbon in the Yukon River and its tributaries: Seasonality and importance of inorganic nitrogen. *Global Biogeochemical Cycles*, *26*(4), GB0E03. https://doi.org/10.1029/2012gb004342

Wickland, K. P., Neff, J. C., & Aiken, G. R. (2007). Dissolved organic carbon in Alaskan boreal forest: Sources, chemical characteristics, and biodegradability. *Ecosystems*, *10*(8), 1323–1340. https://doi.org/10.1007/s10021-007-9101-4

Wilson, S. D., & Nilsson, C. (2009). Arctic alpine vegetation change over 20 years. *Global Change Biology*, *15*(7), 1676–1684. https://doi.org/10.1111/j.1365-2486.2009.01896.x

Xian, F., Hendrickson, C. L., Blakney, G. T., Beu, S. C., & Marshall, A. G. (2010). Automated broadband phase correction of fourier transform ion Cyclotron resonance Mass Spectra. *Analytical Chemistry*, *82*(21), 8807–8812. https://doi.org/10.1021/ac101091w

Yang, M., Yang, Y., Yang, X., Song, X., Du, X., & Lu, Y. (2024). Molecular fingerprinting of the biodegradation of petroleum organic pollutants in groundwater and under site-specific environmental impacts. *Water*, *16*(13), 1773. https://doi.org/10.3390/w16131773

Zimov, S. A., Schuur, E. A., & Chapin, F. S., III. (2006). Permafrost and the global carbon budget. *Science*, *312*(5780), 1612–1613. https://doi.org/10.1126/science.1128908